

**A MINIATURE WIRELESS NEURAL RECORDING AND  
STIMULATING SYSTEM FOR CHRONIC  
IMPLANTATION IN FREELY MOVING ANIMALS**

**By**

**MUSTAFA A. KANCHWALA**

Submitted in partial fulfillment of the requirements of the degree of  
Master of Science

**Thesis Advisor: Dr. Dominique M. Durand**

Department of Biomedical Engineering

**CASE WESTERN RESERVE UNIVERSITY**

August, 2018

**CASE WESTERN RESERVE UNIVERSITY**  
**SCHOOL OF GRADUATE STUDIES**

We hereby approve the thesis/dissertation of

**Mustafa A. Kanchwala**

Candidate for the degree of **Master of Science\***

Committee Chair

**Dr. Dominique M. Durand**

Committee Member

**Dr. Colin Drummond**

Committee Member

**Dr. Pedram Mohseni**

Date of Defense

**June 18, 2018**

\*We also certify that written approval has been obtained for any  
proprietary material contained therein.

## Dedication

*I dedicate this thesis to my family for giving me the opportunity to pursue my dreams, for believing in me and for always standing by my side.*

# Table of Contents

<b>Committee Approval Sheet</b> .....	i
<b>Dedication</b> .....	ii
<b>Table of Contents</b> .....	iii
<b>List of Figures</b> .....	v
<b>List of Tables</b> .....	vi
<b>List of Abbreviations</b> .....	vii
<b>Acknowledgements</b> .....	viii
<b>Abstract</b> .....	x
<b>Chapter 1 Introduction</b> .....	1
1.1 Background .....	1
1.2 Selection of wireless technology .....	2
1.3 Motivation for current study .....	3
1.4 Thesis Objective and Organization .....	4
<b>Chapter 2: A Miniature Wireless Neural Recording and Stimulating System for Chronic Implantation in Freely Moving Animals</b> .....	6
<b>2.1 Introduction:</b> .....	6
<b>2.2 Circuit Design and Implementation</b> .....	7
2.2.1 System Architecture.....	7
2.2.2 Bluetooth Low Energy Microcontroller .....	9
2.2.3 Ultra-wideband – Impulse Radio .....	11
2.2.4 Wireless Neural Recording and Stimulating System .....	13
2.2.5 Receiver Base Station.....	16
2.2.6 System Implementation.....	18
<b>2.3 Measurement Results</b> .....	21
2.3.1 Experimental Validation.....	21
2.3.2 Packet Loss Ratio (PLR) .....	24
2.3.3 Signal to Noise Ratio (SNR) .....	25
2.3.4 Power Measurement .....	26
<b>2.4 Discussion</b> .....	27
<b>Chapter 3 Conclusions and Future Work</b> .....	29

3.1 Conclusion.....	29
3.2 Significance .....	30
3.3 Future Work.....	31
<b>Appendix 1:</b> Device Operation Procedure.....	34
<b>Appendix 2:</b> Data rate of Bluetooth Low Energy (BLE).....	36
<b>Appendix 3:</b> Calculating the Packet Loss Ratio (PLR).....	38
<b>Appendix 4:</b> Bench Tests on a RHD2216 based transmitter.....	41
<b>Appendix 5:</b> Bench Tests on RHS2116 for stimulation .....	43
<b>Appendix 6:</b> Circuit Design Layouts .....	45
<b>Appendix 7:</b> Source Code and PCB Design Files .....	50
<b>References</b> .....	51

## List of Figures

Figure 1: Schematic Diagram of the complete system.....	8
Figure 2: Custom JTAG to Omnetics connector board for programming the implant module .....	10
Figure 3 The UWB frame format for data transmission .....	12
Figure 4: A Block Diagram of the wireless implantable recording and stimulating system .....	13
Figure 5: Implementation of the wireless implantable recording and stimulating system .....	14
Figure 6: Ultra-wideband (UWB) transmission data packet and frame format .....	15
Figure 7: Block diagram of the receiver base station showing the different components .....	16
Figure 8: System Implementation .....	19
Figure 9: Custom modified Intan GUI showing the different buttons.....	21
Figure 10 Experimental setup for validation of the recording system .....	22
Figure 11 Data recorded from implanted CNTY electrodes outside and inside vagus nerve .....	23
Figure 12 Stimulator output measured across a 15K $\Omega$ resistor for a 100 $\mu$ A(pp) biphasic pulse. ..	24
Figure 13: Power measurement performed for the Intan RHD2216.....	27
Figure 14 UWB Frame format for Packet Loss Ratio (PLR) calculation.....	38
Figure 15 Area layout for the PLR test .....	39
Figure 16 Actual setup for the Packet Loss ratio (PLR) measurement.....	40
Figure 17: Experimental setup for testing the RHD2216 recording and transmission system. ....	42
Figure 18: Observed signals at the base station GUI .....	42
Figure 19: Test bench setup for a wired RHS2116. ....	44
Figure 20: Stimulator output as measured across a 15K $\Omega$ resistor.....	44
Figure 21: Schematic of the Implant Module for RHD2216.....	45
Figure 22: layout of the Bottom PCB layer for the Implant module.....	46
Figure 23: Layout of the Top PCB layer for the Implant Module.....	46
Figure 24: Schematic of the Receiver Base Station Shield Board .....	47
Figure 25: PCB layout of the Base Station Shield Board.....	48
Figure 26: PCB layout of the JTAG to Omnetics Converter Programmer Board.....	48
Figure 27: RHS2116 Test Board.....	49

## List of Tables

<i>Table 1: Transmitter Specifications and Performance</i> .....	20
<i>Table 2 Stimulator Current Measurement</i> .....	23
<i>Table 3 Packet Loss Ratio for different transmission distance</i> .....	25
<i>Table 4 Power Measurement for the Implant Module using RHD2216</i> .....	26

## List of Abbreviations

- ksps:** Kilo Samples per Second
- CNTY:** Carbon Nano Tube Yarn
- UWB-IR:** Ultra-wideband Impulse Radio
- BLE:** Bluetooth Low Energy
- PNS:** Peripheral Nervous System
- PNI:** Peripheral Nerve Interface
- MICS:** Medical Implant Communication Service
- IoT:** Internet of Things
- SNR:** Signal to Noise Ratio
- GUI:** Graphical User Interface
- SPI:** Serial Peripheral Interface
- GPIO:** General Purpose Input Output
- FPGA:** Field Programmable Gate Array
- LSB:** Least Significant Bit
- MSB:** Most Significant Bit
- SRAM:** Static Random Access Memory
- PCB:** Printed Circuit Board
- LDO:** Low drop-out regulator
- Li-Po:** Lithium Polymer
- ADPCM:** Adaptive differential pulse-code modulation
- CPLD:** Complex Programmable Logic Device
- LED:** Light Emitting Diode
- OAD:** Over the Air Download



## Acknowledgements

I would like to express my sincerest gratitude to Dr. Dominique Durand, my research advisor and mentor, for his encouragement, guidance and financial support towards this research. I have learned a lot from him beginning from the early days of my first BME course in neural engineering to learning to give better scientific presentations. He has always found the best in me and motivated me to strive for excellence. He allowed me to take a yearlong break from my research to pursue an internship to develop a career in the medical devices industry. He has always supported me in my pursuits and for that I am very thankful to him.

To my committee members, Dr. Colin Drummond for his advice in thinking through the different issues that could arise when this research would be commercialized. It helped me make strategic changes and improvements to the design, and Dr. Pedram Mohseni for his expertise in wireless biomedical systems, for suggesting the key tests to validate the system and improve its overall performance. Their continued support and feedback during the committee meetings helped me stay focused and complete my research.

To my mentor, Dr. Grant McCallum, whose expertise in programming, circuit designing and debugging has helped me come a long way to actually be able to design and implement this project. Without his help in creating the base station program and GUI, this research would not have been possible. His wisdom in always designing with future modifications in mind has helped me finish the project a lot earlier than I anticipated. I

am also very thankful to him for his help in editing this thesis. It is an absolute pleasure to work with him and I am glad to have received his guidance in this journey.

I would like to thank Joseph Marmmerstein for his help in performing animal experiments to validate the system, and advice on processing recorded data and performing calculations on it.

To my family. Mom, dad and brother who have always supported me spiritually, emotionally and financially, they have stood by my side in the tough times and celebrated in my successes. To their sacrifices that have not gone unnoticed, and to their love that has always been my strength.

To my fiancée Fatima who has always believed in me, and has been with me throughout this journey. Her unwavering support has not only helped me get through the tough times, but has made me a better person.

To my cousins, aunt and uncle for their emotional support in these past years, and for being my family in the US.

To my friends in the International Student Fellowship, for motivating me and supporting me.

Thank you all!

# A Miniature Wireless Neural Recording and Stimulating System for Chronic Implantation in Freely Moving Animals

Abstract

by

MUSTAFA A. KANCHWALA

Bioelectronic Medicine Therapies offer a promising alternative to traditional procedures, and implantable devices are crucial for its development. This thesis presents a miniature, low power, 2 channel integrated wireless neural recording and stimulating system with sampling rates of 20ksps to allow researchers to understand the organ functions and develop therapies in freely moving small animals. The wireless implant uses Carbon Nano Tube Yarn (CNTY) electrodes to interface with the peripheral nerves and record signals. High data transmission rates are achieved by using an Ultra-wideband Impulse Radio (UWB-IR) transmitter and wireless switching control is provided by Bluetooth Low Energy (BLE). The UWB transmitter is primarily designed to make it implantable in freely moving rats for long periods of time, to chronically record neural activity in the peripheral nerves and stimulate them wirelessly. Preliminary experiments and bench test results have confirmed its functioning with high data transmission rate and low power consumption.

# Chapter 1 Introduction

## 1.1 Background

Neural activity in the Peripheral Nervous System (PNS) is generally monitored by a Peripheral Nerve Interface (PNI). It is used to record the electrical signals within the nerve to either control external devices and prosthetics, or to identify patterns to help in the monitoring and diagnosis of neurological disorders, ranging from Cardiac arrhythmias and Epilepsy to Parkinson's disease and Depression.[1] the most common use of PNI is in open loop stimulation devices. [2]–[6]

Chronic studies in the PNS are typically performed using either tethered interfaces, or wireless transmission capabilities. The animal could either be anesthetized to eliminate movement artifacts or be freely moving, depending on the study protocol. It has been frequently observed that during tethered chronic studies, the animal bites on the connections, which results in damaged or broken connectors, or risk pulling the connector leading to infection at the site of the percutaneous connector. These issues result in unnecessary delays, loss of implanted animals and unreliable data, and greatly affect the collection of repeatable data for analysis and affect the possibility of long term recordings to monitor progression of activity or treatment administered.

Wireless PNI's are preferred for freely moving animals, and there are several commercially available devices for this purpose that have been used in research studies. However, currently available wireless telemetry devices usually have only two of the

three important components required for functionally implanting in small animals, high data sampling rate, low power consumption and miniature size. Most high data rate wireless devices have a larger footprint and high power consumption, so they are attached onto the animal as backpacks. Other miniature devices have a low sampling rate that is not sufficient to transmit high bandwidth raw neural data for analysis.[7] Even the devices that have a small footprint and high data transmission rates do not have an integrated recording and stimulating system, and an additional stimulator is required.[8]

## 1.2 Selection of wireless technology

There are several options to choose from when selecting a technology for wireless transmission of data from an implantable device. Studies have reported results with the use of Medical Implant Communication Service (MICS) protocol[9][10] and Bluetooth[11][12], [13]. Wi-Fi is another option that is frequently used, due to its high data transmission rates.

With the rise of Internet of things (IoT), wireless technologies like Bluetooth Low Energy (BLE) have provided low power data transmission solutions for many applications that need to send data in small bursts for short distances, with the maximum allowable throughput reaching 1.34Mbps for the latest BLE v5.0 [14] . However, after performing extensive tests and studies using a BLE module described within this thesis, it was found that BLE does not allow real-time, continuous data transmission at sampling rates of 20ksps, and so cannot be used for this application. Instead, a new wireless technology, Ultra-Wideband Impulse-Radio (UWB-IR) is best suited for this application. Ando et al.

provides a comparison of the available technologies and it shows that UWB clearly has an advantage over the existing technologies [15]. UWB is part of the IEEE 802.15.4-2011 protocol and allows higher data rates, low power consumption and a small antenna size which makes it ideal for implantation [16], [17].

### 1.3 Motivation for current study

Chronic neural recordings over long periods of time can allow researchers to better understand the underlying organ functioning and its correlation with neural firing pattern. The primary motivation for this study is to develop the ability to chronically record neural data from freely moving animals and stimulate for longer periods of time.

Due to issues with tethering of wires through percutaneous connectors, collecting chronic neural data in freely moving animals has been very difficult. High risk of infection at the percutaneous connectors can lead to early termination of studies, loss of implanted animals and unreliable data.

Moreover, currently available wireless systems lack the integration of the recording and the stimulating device in a single package, while keeping the footprint and power consumption low to make it implantable without the need to recharge constantly or place it in an inductive chamber to provide continuous power [7], [8].

There is an unmet need for the development of an implantable wireless integrated recording and stimulating device that has a small size, low power consumption and a high data sampling rate to allow transmission of raw neural data and stimulation of the PNS.

## 1.4 Thesis Objective and Organization

The objective of this thesis is to design, build and test a wireless integrated neural recording and stimulating device with a low power consumption, miniature size and a high data sampling rate to transmit raw neural data for processing, and stimulate the nerve.

**Below are the key design specifications used for this system:**

- **Goal:** To design and build an Integrated wireless recording and stimulating device
- **Function:**
  - Record at least 2 channels of neural data at ~20kSamples/sec/channel
  - Stimulate at 1Hz – 10 kHz with a current range of 10nA – 320uA
  - Target recorded signal range between 0.1Hz – 9kHz
- **Power Requirements:**
  - Battery should be rechargeable or should last more than 60 days for a 10 min/day session.
- **Size Requirements:**
  - Should be comparable to or smaller than existing similar devices.  
(Preferably <math> < 9\text{cm}^3 </math>)

This thesis is organized into three chapters. Chapter 1 provides an introduction and sets the premise for the requirement for this study. Chapter 2 presents the proposed solution, discusses the implementation, various components and its performance and the

results obtained in acute animal studies. Chapter 3 provides a conclusion and a glimpse into the future possibilities and opportunities for testing this system and possible improvements.



# Chapter 2: A Miniature Wireless Neural Recording and Stimulating System for Chronic Implantation in Freely Moving Animals

## 2.1 Introduction:

Bioelectronic Medicine is a promising alternative to treat diseases without the use of traditional drugs. These devices interface with a nerve to record and manipulate its electrical activity. By recording these signals and identifying the underlying patterns it might be possible to treat a wide range of neurological disorders from cardiac arrhythmias and epilepsy to Parkinson's disease and Depression[1].

Implantable systems will play a key role in the development of closed loop Bioelectronic Medicine therapies, however, while there are several implantable stimulators and recorders in the market, there are very few fully integrated implantable recording and stimulating systems that have high data transmission rates, low power consumption and a miniature size. The existing high bandwidth recording systems are mostly external, and utilize tethered wires for connecting to the electrodes. This increases the risk of infection due to percutaneous connections and movement [18]. Those systems that are small enough to be fully implanted do not have sufficiently high data transmission rate to transmit raw, real-time neural data at high sampling rates, and even these systems do not have an integrated stimulator to make a closed loop system. These issues can be addressed by developing a fully implantable wireless integrated recording and stimulating system with a high data transmission rate, low power consumption and a very small size,

to analyze the neural signals for patterns associated with neurological disorders that can be manipulated by stimulating the nerves in a closed loop system.

This thesis presents a 2 channel wireless recording and stimulating system with a sampling rate of 20ksp/s/channel that can be implanted to chronically record neural data and stimulate the implant site in a freely moving rat. The system uses an Ultra-wideband Impulse Radio (UWB-IR) based transmitter to transmit raw data to a receiver connected to a host computer, with a BLE based control to start and stop the recording and stimulation of the nerve. UWB technology is used for transmission of raw data due to its high data rate and low power consumption that makes it best suited for this application [15].

## 2.2 Circuit Design and Implementation

### 2.2.1 System Architecture

The wireless telemetry system shown in Figure 1, consists of an implant module (Figure 1a) that records neural signals and stimulates the nerve, and a receiver base station (Figure 1b) that is connected to a host computer to control the recording and stimulation and to display and store the recorded data. The implant module uses a low noise single ended biopotential amplifier and stimulator chip RHS2116 from Intan Technologies, LLC [19] that is interfaced with the Carbon Nano Tube Yarn (CNTY) electrodes to provide a very flexible and low impedance interface to measure the neural signals [20].

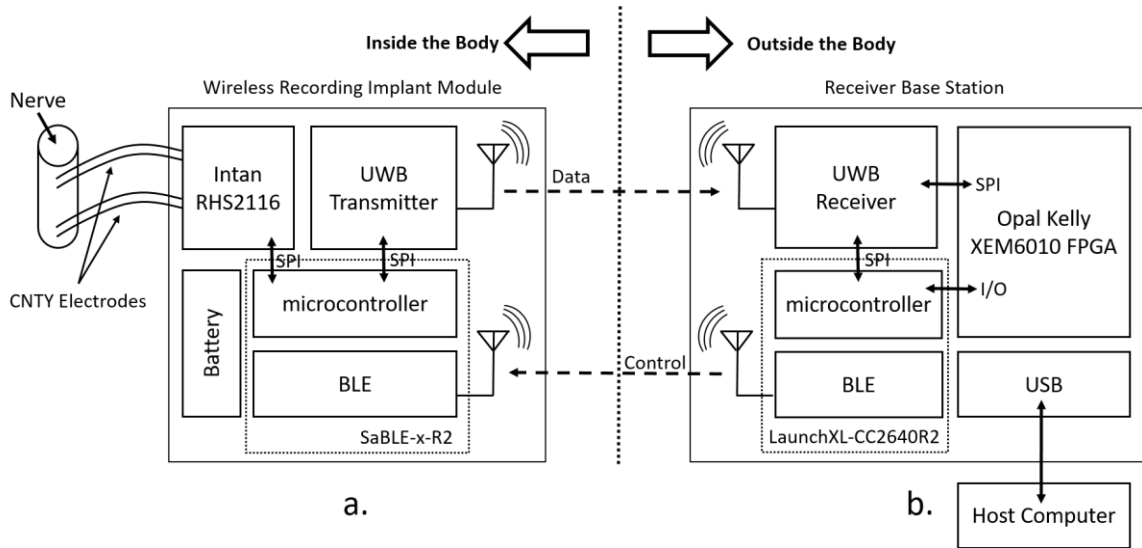


*Figure 1: A Schematic Diagram of the complete system, where (a) shows the wireless implantable recording module with the Intan RHS2116 that records from and stimulates the CNTY electrodes implanted in the nerve. It is battery powered and controlled by a BLE connection to the base station. UWB is used to transmit the raw neural data. (b) Shows the Receiver base station that is connected to the host computer GUI to control the implant using BLE. The UWB receiver works in sync with the FPGA board to collect and process the incoming data which is displayed on the GUI.*

The Intan RHS2116, digitizes the signals and interfaces with a TI CC2640R2F [21], a 32-bit microcontroller with an integrated BLEv5 radio core that is used for collecting and processing the data. The BLE connection controls the operation of the implant from the host computer's user interface. Once the data is collected and hardware averaged to further improve the SNR [22], it is packaged into a series of 30 samples ready for wireless transmission to the receiver using a DecaWave DWM1000 Ultra-wideband Module [23]. On the receiver side, the microcontroller CC2640R2F continuously polls the status flag of the Ultra-wideband receiver for the data packets and once data is received, the XEM6010 FPGA [24] state machine fetches and stores this data, which is displayed on the modified Intan GUI and can be stored in the host computer for further processing. For stimulating

the nerve, the user sends start and stop stimulation commands from the host computer GUI.

### 2.2.2 Bluetooth Low Energy Microcontroller

To select a microcontroller for the implant module and the receiver base station, the desired features are to have a low power microcontroller with a high-speed Serial Peripheral Interface (SPI) for connecting with the Intan RHS2116 amplifier chip to provide high data sampling rate. A Bluetooth Low Energy (BLE) core integrated within to allow controlling the system wirelessly, sufficient I/O pins and a low overall footprint suitable for implantation in rodents. The best option for this application was found in Texas Instruments' CC2640R2F. A 32-bit ARM Cortex M3 microcontroller with an on-chip Bluetooth Radio Core. The Bluetooth radio supports Bluetooth Low Energy (BLE v4.2) and is also compatible with the latest Bluetooth 5 release. With a 48 MHz system clock and a maximum SPI rate of 12MHz, this microcontroller can easily interface with the RHS2116 and DWM1000 modules to perform quick data transfer while maintaining the high data sampling rates. Moreover, Laird Technologies manufactures an integrated module (SaBLE-x-R2) [25] that integrates a CC2640R2F and the associated RF circuitry in a FCC compliant package that makes it easier to use for quick development without having to debug issues with the RF circuit design. All these features made this microcontroller the best candidate for this application.

The Transmitter implant board uses a SaBLE-x-R2 module for data acquisition, processing and for the BLE control, while the Receiver base station uses a CC2640R2-LaunchXL

development board from Texas Instruments due to the availability of 15 additional I/O pins that allow the microcontroller to be interfaced with the FPGA and the DWM1000 module, and to allow debugging.

The CC2640R2-LaunchXL board has a XDS110 debugger onboard that allows debugging the receiver program. It can also be connected to the implant module using a JTAG cable and a custom programmer board developed to interface the JTAG pins to the Omnetics pins on the implant board. Figure 2 shows the setup with the JTAG cable connected to the programmer board and another cable connects it to the implant board. This Board is a component of the Receiver Base Station and is used for BLE communication with the implant, programming the UWB receiver, and coordinating data reception with the FPGA board.

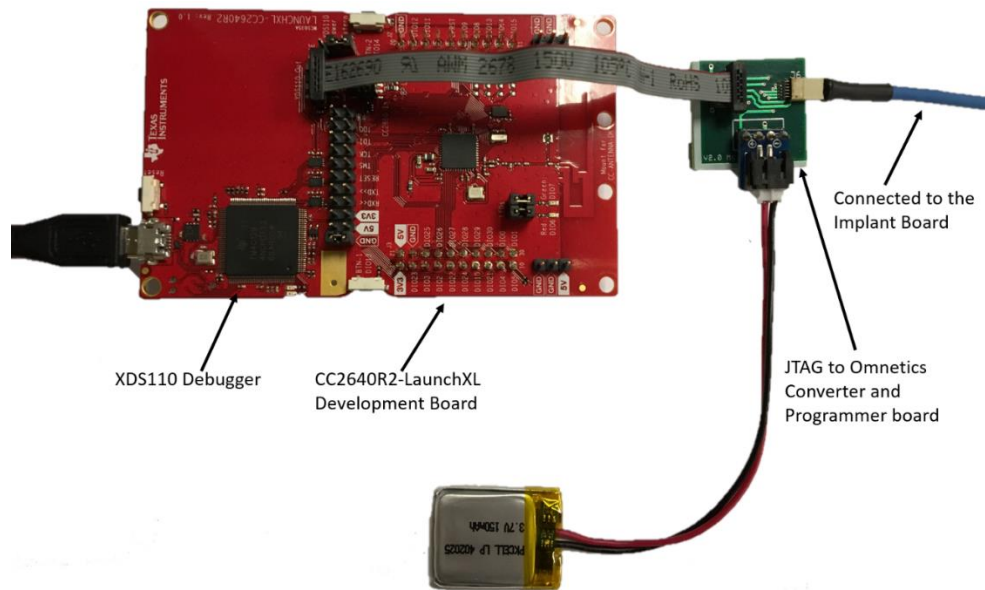


*Figure 2: The CC2640R2-LaunchXL development board connects to the custom JTAG to Omnetics connector board that is built to allow programming and debugging capabilities for the implant module.*

### 2.2.3 Ultra-wideband – Impulse Radio

Of the several wireless technologies available today, the Ultra-wideband Impulse Radio (UWB-IR) is best suited for this application as it has all the necessary features like very low power consumption, high data transmission rate and small antenna size that are needed for an implantable system for the transmission of raw neural data. Ando et al. [15] provides a comparison of different wireless technologies currently available.

DecaWave has a commercial UWB transceiver chip (DW1000) based on the IEEE 802.15.4-2011 standard [26] that provides a configurable UWB transceiver that can be used in operational data rates of 110Kbps, 850kbps and 6.8Mbps. Lower data rates allow longer range of communication due to increased length of preamble. DecaWave also manufactures the DWM1000 module that incorporates the DW1000 chip with the required RF circuitry and a ceramic omnidirectional chip antenna. This module is used for the current application to avoid any issues due to RF circuit designing. It is currently used at a maximum data transmission rate of 6.8Mbps, which includes the data payload as well as the preamble and frame format bits. It is well suited for the transmission of 2 channels of raw neural data sampled at 20ksps/channel.

On the transmitter implant, a DWM1000 module is used as a dedicated UWB transmitter. The CC2640R2F microcontroller stores the data acquired from the Intan RHS2116 in the transmission buffer of the DWM1000 module, and then initiates a transmit command to transmit the data to the receiver.

On the receiver base station, another DWM1000 acts as a dedicated UWB receiver and stores the received data in its receive buffer that is read by the FPGA for processing and display.

The transmit and receive memory buffers on the DWM1000 can only hold 8 bit data (or 1 Byte), due to limited buffer depth. This requires the 16-bit data samples from the Intan RHS2116 to be split into the 8-bit MSB and 8-bit LSB components before transmission. It works in Slave SPI mode and its maximum operational SPI rate is 20MHz. However, as the maximum achievable SPI rate of the microcontroller is only 12MHz, it is used at 12MHz for this application.

The DWM1000 follows a customizable frame format as described in the IEEE 802.15.4-2011 standard. For this application, as shown in Figure 3, the frame format uses a 64 symbols Preamble, 8 symbols for the Start of Frame Delimiter (SFD), 21 bits for the Physical Header (PHR), and a data payload of 127 bytes, of which this application uses 126 bytes.

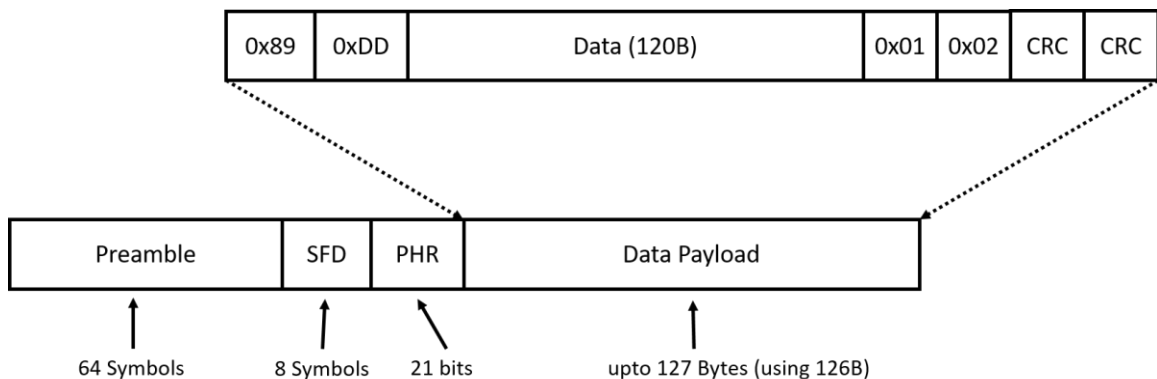


*Figure 3 The UWB frame format for data transmission from the DWM1000 of the implant module. It includes the Preamble, the Start of Frame Delimiter (SFD), the Physical Header (PHR) and the Data payload.*

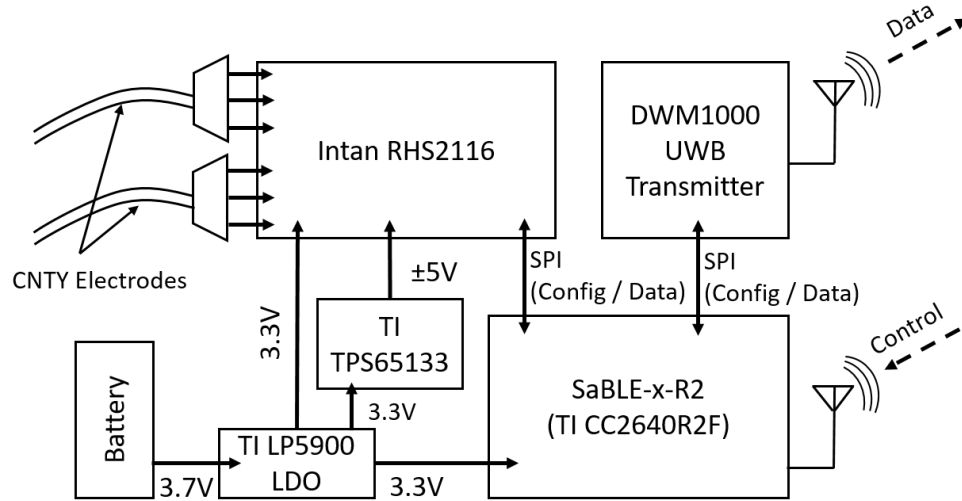


*Figure 4: A Block Diagram of the wireless implantable recording and stimulating system showing the different components. The entire system is powered by a battery. A low dropout regulator (LDO) and a dual output power supply provide the required voltage levels. Control commands are received by the BLE microcontroller (SaBLE-x-R2) which triggers the Intan RHS2116 to record from or stimulate the electrodes. The UWB transmitter transmits the recorded data back to the base station for processing.*

#### 2.2.4 Wireless Neural Recording and Stimulating System

Our proposed two channel neural recording and stimulating system block diagram shown in Figure 4 and implementation in Figure 5 uses an integrated 16-channel low noise single ended amplifier and stimulator chip from Intan Technologies, LLC (RHS2116) to record the neural signals and stimulate the nerve. It is interfaced with the SaBLE-x-R2 BLE module that collects the data and interfaces with a DWM1000 Ultra-wideband module to transmit the recorded raw neural data to the receiver. The implant is controlled by the receiver GUI and commands are sent wirelessly to the SaBLE-x-R2 using BLE. This setup is powered by a 150mAh Li-Po rechargeable battery, and a TI LP5900 ultra-low noise Low Dropout Regulator (LDO) [27] is used to convert the 3.7V from the battery to a regulated 3.3V



supply. To have a  $\pm 5V$  supply for the stimulator, a TI TPS65133 Dual Output Power Supply [28] is used.

The different components work together in synchronization starting with the RHS2116, where the first 3 amplifier channels are tied together to form the first input, and the next 3 channels are tied together to form the second input. This allows us to perform hardware averaging to improve the Signal to Noise Ratio (SNR) [22]. These two inputs could be connected to the Carbon Nano Tube Yarn (CNTY) electrodes [20], as these electrodes are biocompatible, flexible, have low impedance, and have demonstrated chronic neural recordings.

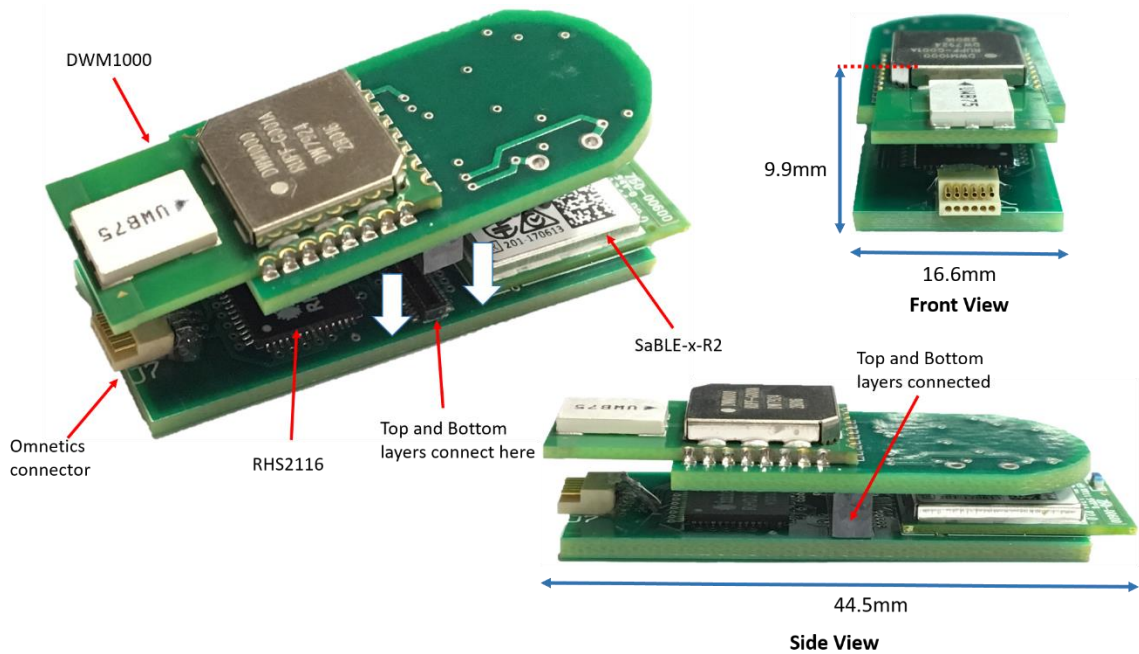


*Figure 5: Implementation of the wireless implantable recording and stimulating system. The top PCB has the DWM1000 UWB module and the power supply circuit, and the bottom PCB has the RHS2116 and the SaBLE-x-R2 microcontroller. The two layers are connected together by a board-to-board connector as shown. The electrodes and battery are connected to this device using the Omnetics connector.*

The RHS2116 amplifies and digitizes the signals with a 16 bit resolution. The SaBLE-x-R2 interfaces with the RHS2116 and acquires the data at a sampling rate of 20ksp/s/channel, using a Serial Peripheral Interface (SPI). This data is stored in a buffer and hardware averaging is performed by the microcontroller using 3 channels on both inputs. Every 16 bit averaged sample is then split into the higher 8 bits (MSB) and the lower 8 bits (LSB) and then stored in the transmit buffer of the DWM1000 UWB module using the SPI interface.

A single transmission packet is ready when 30 data samples from both channels have been stored in the transmit buffer of the DWM1000 in the frame format shown in Figure 6. At this point, the microcontroller triggers the transmission of this packet by sending the transmit command over the SPI interface to the UWB module.

This process repeats every 30 samples and sends data packets wirelessly to the receiver.

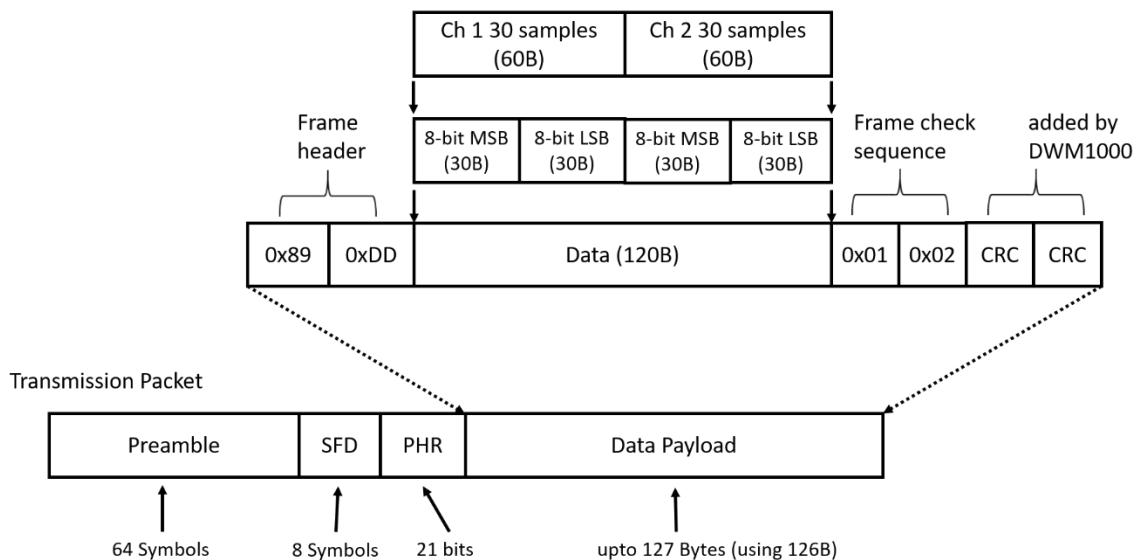


Figure 6: Ultra-wideband (UWB) transmission data packet and frame format. It shows the data from the 2 channels split into the 8-bit MSB and LSB and added to the Data segment of the Transmission Packet Data Payload.

The stimulator is controlled by the receiver base station via the host computer GUI. When the user starts the stimulator, a predefined pattern that is programmed in the implant generates a stimulator pulse train that continues to stimulate the nerve until the Stop button is pressed on the GUI. Data recording is disabled when the stimulator is operational, and once the stimulator is turned off, recording can resume.

### 2.2.5 Receiver Base Station

The receiver performs bidirectional communication between the implant module and the User Interface on the host computer. It allows the user to connect to the implant module and control its operation for recording and stimulation using inputs from the GUI. When the implant is transmitting neural data, the receiver collects it, and sends it to the host computer GUI to display and store on the computer.

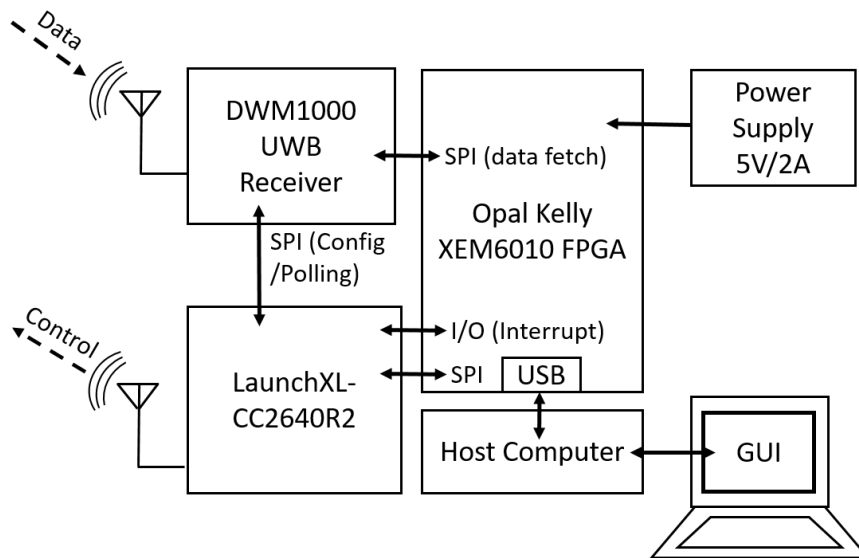


Figure 7: Block diagram of the receiver base station showing the different components. The GUI on the host computer sends control commands using BLE to the implant board to record data or stimulate. The recorded data is received by the UWB receiver, and is transferred to the FPGA board for processing and display on the GUI.

The receiver base station shown in Figure 7 uses a CC2640R2-LaunchXL development board with the CC2640R2F microcontroller. An Opal Kelly XEM6010 FPGA board interfaces with the microcontroller via SPI and the host computer using a USB connection. This interface allows communicating with the GUI to display and store the data collected by the FPGA from the DWM1000 UWB receiver module.

Control commands to the implant for recording and stimulation are sent from the GUI to the BLE microcontroller via the FPGA interface. The BLE radio sends these commands wirelessly to turn the recording and stimulation ON or OFF. When the recording is turned ON, the UWB module on the receiver is actively waiting to receive the data packet. The microcontroller continuously polls the status flag of the DWM1000 and generates an interrupt when the receive flag is set. This signals the FPGA module to initiate the data fetch state machine to collect the data from the receive buffer of the DWM1000. Once the data is collected by the FPGA, it signals the microcontroller of a successful fetch and the microcontroller returns to polling for data packets again. The data collected is converted back to 16 bit samples by merging the 8 bit MSB and LSB, and is stored in the SRAM of the FPGA. This data is ready to be displayed by the modified Intan user interface software RHD2000 Series v1.5.2 (open source software provided by Intan Technologies, LLC) that collects the data from the SRAM at 20ksps sampling rate, and displays it onto the GUI and stores it.

## 2.2.6 System Implementation

Figure 8 (a) Shows the wireless implant module and figure 8 (b) shows the receiver base station. The implant module is implemented using 2 PCB boards attached together with a DF40C-60DP-0.4V(51) (Header) and DF40HC(4.0)-60DS-0.4V(51) (Receptacle) board-to-board connector from Hirose Electric Co. Ltd. The bottom PCB holds the Intan RHS2116 chip and the SaBLE-x-R2 module. It includes a 12-pin Omnetics PZN-12-AA connector that connects to a JTAG programmer board for programming and debugging as shown previously in Figure 2. The Top PCB has the DWM1000 UWB module, the TI LP5900 LDO to convert the battery voltage (3.7V) to a regulated 3.3V to power the different components and the TI TPS65133 Dual Output Power Supply to have a  $\pm 5V$  output to provide power to the stimulator power supply on the RHS2116. These two layers are then attached together using a board-to-board connector, as shown in Figure 5.

Once programmed, the JTAG connector is removed and replaced with another connector that connects the electrodes and battery to the implant board, which is then encapsulated with medical grade biocompatible epoxy (EPO-TEK MED-301, Epoxy Technology). A 150mAH Li-Po rechargeable battery is used to power the implant board, and is encapsulated in a separate package. Table 1, summarizes the system specifications and performance. A percutaneous plug is currently used to recharge the battery when needed, however, it can be replaced by a wireless recharging circuit in the future, to make the device fully implantable.

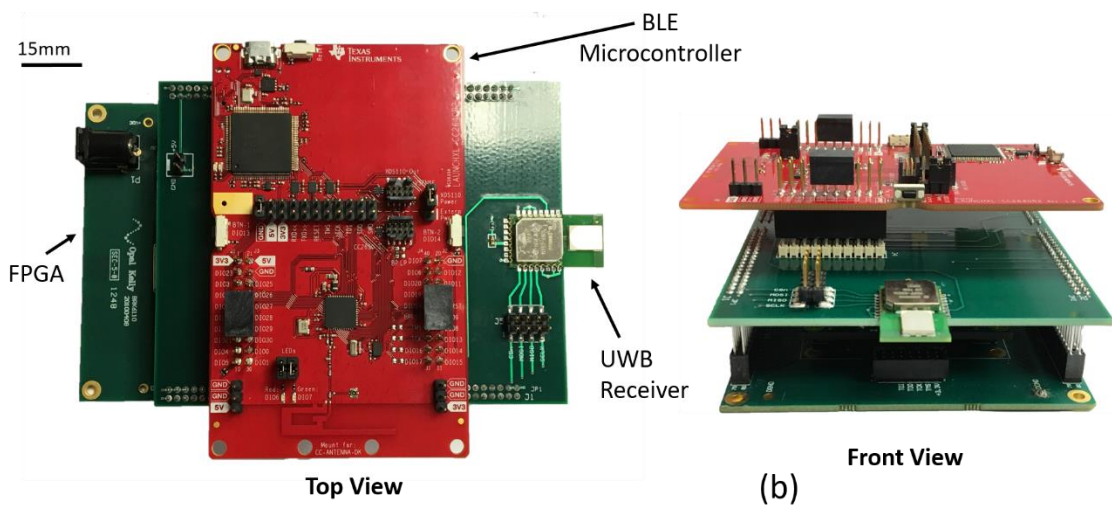
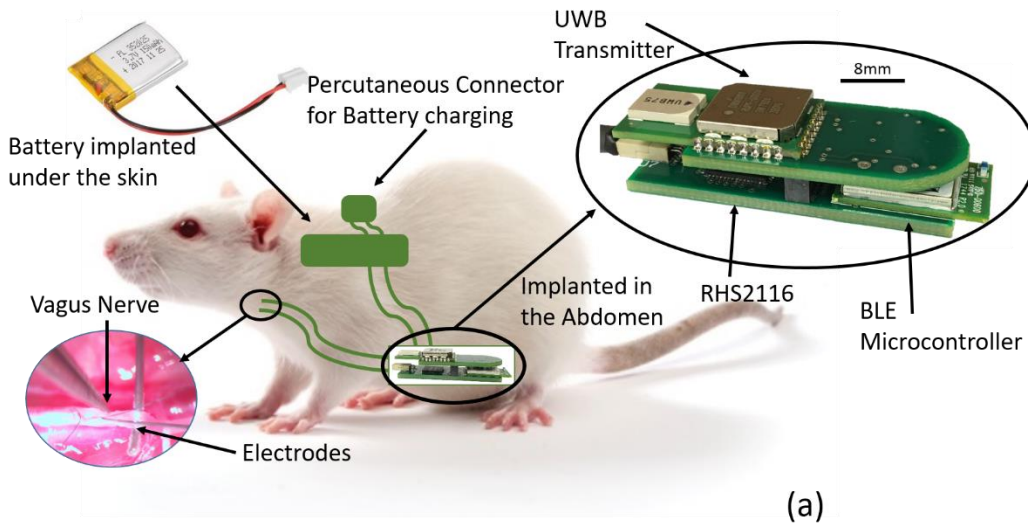


Figure 8: System Implementation. (a) Shows the 2-channel wireless recording and stimulating module that can be implanted in the abdomen of a rat, with the electrodes in the vagus nerve. A percutaneous port is used to recharge the battery that powers the implant. (b) Shows the receiver base station and the different components used in its assembly. The base station connects to the host computer via a USB.

The receiver base station shown in Figure 8(b) uses a XEM6010 FPGA board mounted on the BRK6110 board to allow access to its I/O pins. A custom PCB board with the DWM1000 UWB module is interfaced with it, and the CC2640R2F LaunchXL board is mounted on top.

The entire setup is powered by a 5V 2A power supply, and it is connected to the host computer using a USB connection.

*Table 1: Transmitter Specifications and Performance*

<b>System Parameter</b>	<b>Value</b>
Number of channels	2
Recorded Bandwidth	100Hz – 5kHz
Sampling Frequency	20ksps
Sample Resolution	16 bit
Stimulator Current Step Size	10nA <sub>(min)</sub> – 10uA <sub>(max)</sub>
Stimulator Current Range*	10nA <sub>(min)</sub> – 166uA <sub>(max)</sub> @ ±5V
Telemetry Frequency	6.4GHz
Power Supply	3.7V
Battery Life**	~6Hrs
Max Power Dissipation (3.3V)	84.14 mW
Transmission Range***	>5m
Dimensions***	44.5 x 16.6 x 9.9mm <sup>3</sup>
Weight***	6.87gm

\* - with a ±5V supply across an electrode impedance of ~15kΩ

\*\* - with a 150mAh battery

\*\*\* - without encapsulation

The host computer runs a custom-modified version of the Intan RHD2000 Series v1.5.2 GUI, where additional buttons have been added such as “Init BLE” to reset the Bluetooth microcontroller, and “Stim\_START” and “Stim\_STOP” to control the stimulation. Init BLE resets the microcontroller using the GUI to initiate a new connection to the implant to

establish control for recording and stimulation and receive the raw neural data. Figure 9 shows the modified GUI buttons.

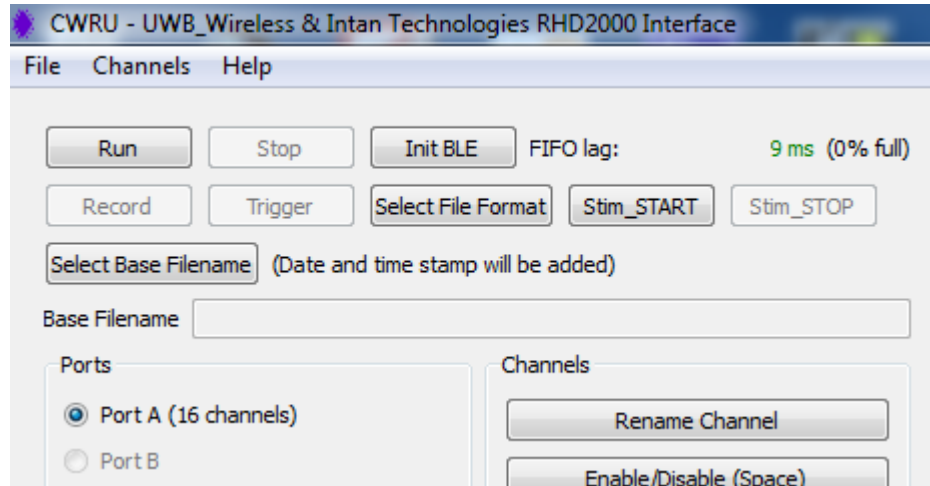


*Figure 9: Custom modified Intan GUI showing the Init BLE button to establish a connection to the transmitter. The Run, Record and Stop buttons to control the recording, and the Stim\_START and Stim\_STOP buttons to control the stimulation.*

## 2.3 Measurement Results

### 2.3.1 Experimental Validation

To validate the recording system, acute animal experiments are performed on an Adult male Sprague Dawley rat (350–450 grams, Charles River Laboratories) by connecting the transmitter module to the percutaneous connector on its back. This rat is chronically implanted with 4 CNTY electrodes. 2 electrodes are implanted next to the left cervical vagus nerve (channel 1) and 2 are implanted inside the left cervical vagus nerve (channel 2). The rat is anesthetized with 2% isoflurane in 1L/min oxygen. The overall experimental setup is shown in Figure 10. Data is recorded differentially at 20ksps/ch using the wireless



transmitter module and is shown in Figure 11. Channel 1 clearly shows ECG signal activity that is recorded by the electrodes implanted outside the nerve, while no other significant activity is recorded. In comparison, channel 2 shows the vagus nerve activity that corresponds to the breathing cycle, as recorded by the electrodes implanted inside the nerve. After a 20 minute recording session with the wireless transmission system, an Intan RHD2216 wired recording system was attached to the anesthetized rat, and data from the electrodes was recorded and compared. The wirelessly recorded data was found comparable to that observed using a wired Intan RHD2216 system on the same animal.

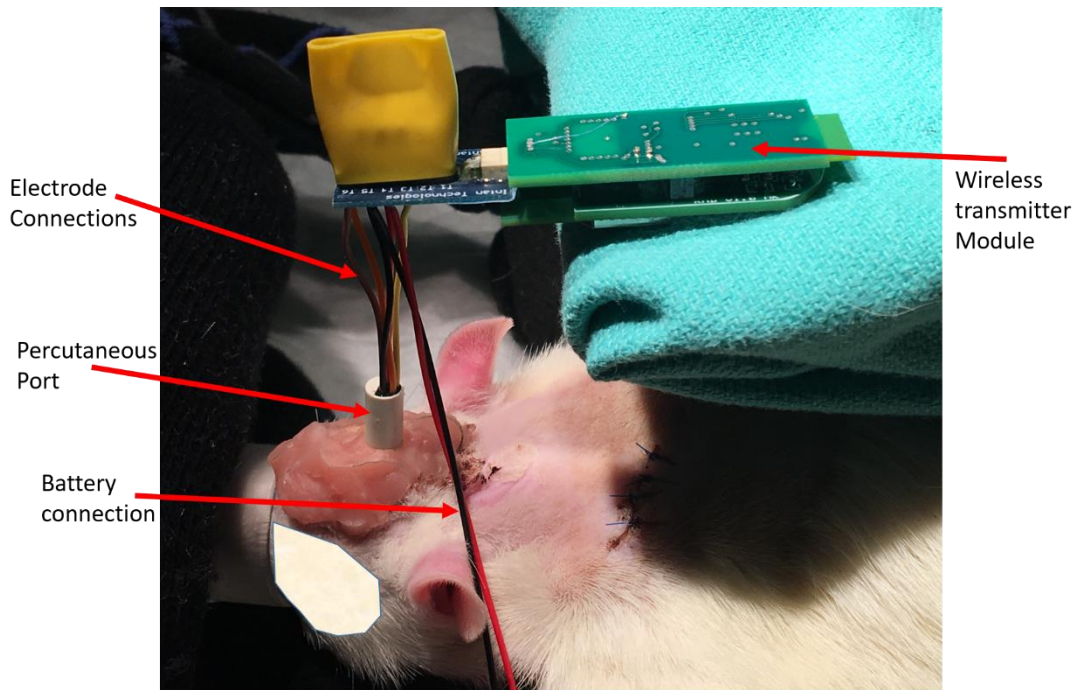


*Figure 10 Experimental setup for validation of the recording system. The wireless transmitter module is connected to the percutaneous port of an anesthetized rat, using a custom connector. The rat is implanted with 4 CNTY electrodes, with 2 electrodes next to the left cervical vagus nerve and 2 electrodes inside the left cervical vagus nerve. The module is battery powered, and transmits the data to the base station for processing and storing in the memory.*

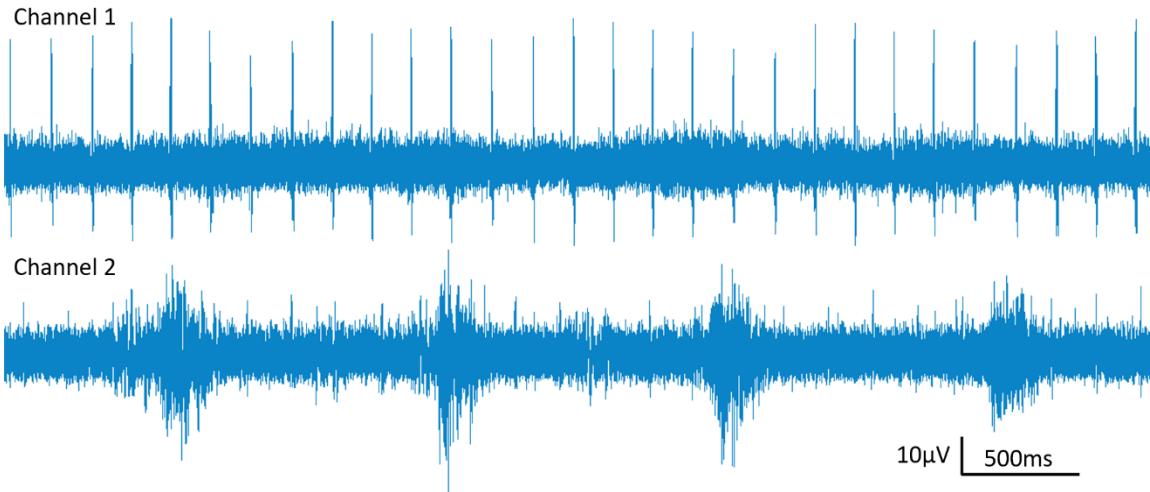


*Figure 11 Data recorded from CNTY electrodes implanted outside the left cervical vagus nerve (Channel 1) and inside the left cervical vagus nerve (Channel 2) using the wireless UWB transmitter. Channel 1 shows ECG signal that is picked up by the external electrodes, while channel 2 records the vagus nerve activity that corresponds to the breathing cycle of the anesthetized rat.*

The wireless stimulator control circuit is validated on a test bench, by using a predefined stimulation parameter value (biphasic pulse train with  $100\mu\text{A}_{\text{pp}}$  at  $1\text{KHz}$  frequency) that is programmed to the implant module microcontroller. When the stimulation is triggered from the host computer GUI, The stimulation pulse train output is measured across a  $15\text{k}\Omega$  resistor to simulate the impedance of a CNTY electrode in the nerve. Figure 12 shows the stimulation waveform that is measured. Table 2 shows the measurements performed on the stimulation pulses compared to the programmed parameters.

*Table 2 Stimulator Current Measurement*

	<b>Negative Current (<math>\mu\text{A}</math>)</b>	<b>Positive Current (<math>\mu\text{A}</math>)</b>
<b>Programmed Value</b>	-50	50
<b>Measured Value</b>	$-51.46 \pm 0.42$	$48.03 \pm 0.90$
<b>Confidence %</b>	97.06%	96.06%

The integrated recording and stimulating transmitter system is validated by wirelessly connecting to it from the base station and then recording and stimulating for 10 minute sessions, to ensure that connectivity to the base station and the GUI is maintained and the system can be wirelessly controlled.

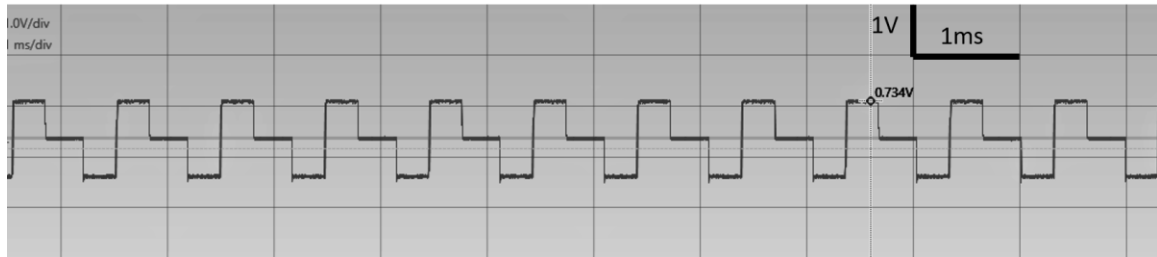


*Figure 12 Stimulator output measured across a 15K $\Omega$  resistor for a 100 $\mu$ A(pp) biphasic pulse at 1Khz frequency. 15K $\Omega$  resistor is used to simulate the impedance of a CNTY electrode.*

### 2.3.2 Packet Loss Ratio (PLR)

The data transmitted from the DWM1000 module is packetized into a frame format as shown in Figure 3 and Figure 6. Whenever a packet is corrupted during transmission either due to incorrect format, or due to a bit error, the entire packet gets discarded. So a good measurement to identify transmission efficiency is Packet Loss Ratio (PLR).

A series of tests are performed at different distances between the transmitter and the receiver using a predefined transmission data packet that has a packet counter and a series of alternating zeros and ones. This data is recorded at the base station and

analyzed to find any missing packets. The results are presented in Table 3, that show a very low PLR percentage.

*Table 3 Packet Loss Ratio for different transmission distance*

<b>Transmission Distance (m)</b>	<b>Total Packets</b>	<b>Dropped Packets</b>	<b>Packet Loss Ratio (PLR)</b>	<b>Packet Loss Ratio (PLR) %</b>
0.1	3630	0	0	0
1	3631	0	0	0
2	3630	1	$0.275 \times 10^{-3}$	0.0275
3	3632	1	$0.275 \times 10^{-3}$	0.0275
4	3629	3	$0.826 \times 10^{-3}$	0.0826
5	3625	0	0	0

It is found that the UWB packets can bounce back from metal surfaces and reach the receiver base station before an actual transmitted packet can be received. This results in a lost packet, however a very small fraction of the total packets actually had incorrect bits that resulted in the packet getting discarded by the UWB receiver.

### 2.3.3 Signal to Noise Ratio (SNR)

The SNR for the wireless transmitter is calculated by measuring the average signal power during neural activity in the vagus nerve that corresponds to the breathing cycles divided by the average signal power when there is no activity present. This process was repeated for 5 different measurements performed on the recorded data and the result was converted to decibels. The average SNR was found to be  $7.1 \pm 0.9$  dB.

### 2.3.4 Power Measurement

Power measurement calculations are performed for the individual modules of the implant (Table 4) (with the Intan RHD2216 chip), as well as for the entire system using a TI INA216 current shunt monitor chip [29]. A  $0.15\Omega$  resistor is used as shunt, and the INA216 has a gain of 100. The voltage measured is shown in Figure 13. Using the voltage measurements, current values are calculated and averaged over a 1 second period. Power is calculated using a 3.3V source. The results show that the implant module is a low power device that consumes only  $72.4 \pm 3.4$  mW power when recording the signals and transmitting the data. This is due to low power operation of the UWB module which consumes large currents only when transmitting data for short period of time, as shown in figure 13. A battery life of approx. 7 hours was estimated for continuous recording and transmission based on calculations and experimental power consumption data using a 150mAh Li-Po battery.

*Table 4 Power Measurement for the Implant Module using RHD2216*

<b>Component</b>	<b>Avg Current Measurement</b>	<b>Power</b>
CC2640R2F	$9.776 \pm 1.2$ mA	$32.26 \pm 4$ mW
Intan RHD2216	$2.043 \pm 0.7$ mA	$6.74 \pm 2.3$ mW
DWM1000	$10.12 \pm 1.0$ mA	$33.396 \pm 3.3$ mW
<b>Total</b>	<b><math>21.939 \pm 1.03</math> mA</b>	<b><math>72.4 \pm 3.4</math> mW</b>

\* - Similar calculation can be performed for the Intan RHS2116.

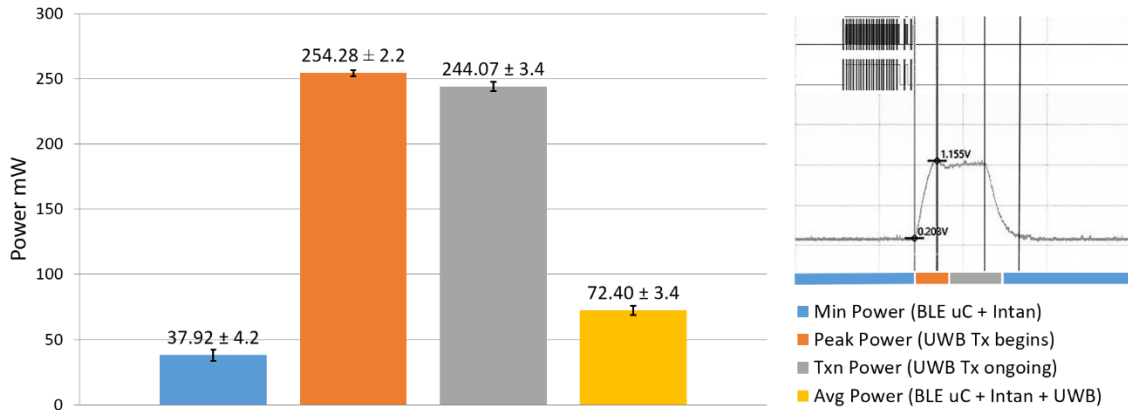


Figure 13: Power measurement performed for the Intan RHD2216 based transmitter system using TI INA216 current shunt monitor with a gain of 100. The voltage measured across the 0.15Ω shunt resistor is shown in the top right corner. Power consumption is very low for the most part during data recording. It increases momentarily during the UWB transmission, before returning back to the low power state.

## 2.4 Discussion

A low power integrated wireless neural recording and stimulating system is presented that can record 2 channels of raw neural data at 20kps from electrodes implanted in a nerve and can stimulate the implant site with a predefined stimulation parameter.

This device paves the way for developing a fully implantable system that could be very useful in the development and testing of bioelectronic medicine therapies in small animal models. It could allow researchers to monitor neural activity and modify it in a closed loop system to better understand the correlation between underlying organ functioning and neuronal firing pattern.

The device presented here uses an UWB – IR based transmitter to wirelessly transmit raw neural data at sampling rates of 20kps/channel. It is controlled by a custom GUI interface on a host computer that interfaces with a BLE microcontroller to allow the user to

wirelessly control the recording and stimulation on the implantable device. This device has low power consumption and can operate continuously for up to 7 hours using a 150mAh battery.

Acute animal experiments are performed on this system using a chronically implanted rat with CNTY electrodes in the left cervical vagus nerve. Data is recorded at 20ksps/channel and the results obtained are very promising with an SNR of  $7.1 \pm 0.9$  dB and comparable to the data seen on a wired system with the same sampling rate. A simulated test with the impedance comparable to a CNTY electrode showed good results with the stimulator, and the stimulation current values were consistent with the programmed parameters with a 96% confidence level. Chronic studies in rodents can be performed to further study the system performance.

## Chapter 3 Conclusions and Future Work

In this chapter, conclusions drawn from chapter II are discussed as they relate to the goal of this thesis to develop an integrated wireless neural recording and stimulating device to interface with the peripheral nervous system in freely moving animals.

### 3.1 Conclusion

The first prototype of an integrated wireless neural recording and stimulating device has shown very promising results. It has also achieved the key design objectives that are required to make it a low power implantable device. Below is an analysis of its capabilities and shortcomings.

- **Goal:** The Goal to design, build and test an integrated wireless neural recording and stimulating system has been fulfilled with this device. It has wireless control using Bluetooth Low Energy (BLE) based connection, and the data is transmitted and received using Ultra-wideband Impulse Radio (UWB-IR) protocol. Preliminary test results have clearly shown that this device has a potential to become a fully implantable wireless system.
- **Function:** This device is capable of recording 2 channels of raw neural data at 20ksps/channel for a signal range of 0.1Hz – up to 10kHz. However to reduce the noise, the internal filtering is programmed for an effective bandwidth of 100Hz to 5kHz. It can also stimulate the electrodes with a programmable stimulation



current value between 10nA – 320µA from 1Hz – 10kHz, and provides a sufficient range to allow stimulating the nerves and blocking.

However, the current prototype only allows the user to program one stimulation parameter at a time. To change the stimulation value, the device needs to be reprogrammed.

- **Power Requirements:** Power measurements performed on RHD2216 system and estimated for the RHS2116, shows that this device can operate continuously for up to 7 hours for a recording only system and up to 6 hours for a recording and stimulating system. The battery is rechargeable, however it still needs to be connected externally to recharge. A percutaneous connector can be used to recharge it if the device is implanted in the current state.
- **Size Requirements:** The overall volume of the transmitter without the encapsulation is about 7.3 cm<sup>3</sup>, which is smaller than other commercially available devices [7].

## 3.2 Significance

The results obtained are very promising in the pursuit to create a wireless fully implantable integrated recording and stimulating device that can record raw neural signals from multiple channels at high sampling rates and stimulate the implant site, while consuming low power and having a small size to facilitate chronic implantation for long term studies in freely moving small animals. Additional work that can be done to improve the current prototype design are mentioned in the next section.

### 3.3 Future Work

The wireless transmitter device in its current state is not implantable, and to make it implant ready, two tasks need to be performed:

1. Encapsulate the system in a biocompatible epoxy to make it implantable.
2. Implant the device in a rat for a chronic study to validate the system.

In terms of system performance, there are several key areas, where design improvements could be made to maximize the performance of the current system and increase the number of recording / stimulating channels beyond the initial 2 channels proposed in this thesis.

Below is a list of activities to perform that can help in validating the system and improve its overall performance.

**1. Histology:** To better understand the impact of a high frequency RF transmitter placed close to skin and body, a comparison study of the cells in an animal with the implant and without the implant can be performed to identify any cell damage caused by exposure to RF transmission due to close proximity to the UWB transmitter.

**2. Different receiver antenna:** Another test would be to identify the performance of the receiver when using different antennas, like Horn antenna, omnidirectional chip antenna and whip antenna. This could help to identify the optimal combination of receiver sensitivity and transmission power that allows optimization of battery life for the overall system.

**3. Effect of motion:** Current bench tests were unable to replicate actual working conditions for the implant, and to establish the noise immunity of the system, this device can be tested under scenarios that induce motion artifacts in normal systems, to see if these could be avoided in the wireless implantable system. Tests could be performed to intentionally induce motion artifacts and see the impact on the data transmitted.

**4. UWB interference:** Preliminary acute studies showed that the UWB transmitter induces noise in the recording system when it is in close proximity to the RHD2216 / RHS2116. To ensure that the system works free from that noise contamination, as well as in scenarios where there are multiple UWB transmitters, Tests can be performed to identify the source of interference and the best solution possible to avoid this noise from affecting the recorded data.

**5. Encapsulation:** To make the device implant ready, it needs to be encapsulated. However, as the medium around the antenna changes from air to the encapsulation material, the antenna characteristics might change resulting in detuning of the antenna. To make sure the antenna tuning is corrected, tests need to be performed with different encapsulation materials to identify the best encapsulation that does not affect the antenna characteristics, or if needed, to perform antenna tuning calibration.

Apart from that, there are a few hardware or software changes can be made to improve the system performance and increase the number of channels.

**1. ADPCM:** Using ADPCM with 4:1 software compression, as shown in [30] and [31], could allow recording from 8 different channels simultaneously using the same hardware

configuration. ADPCM encodes the acquired data with a 4:1 compression ratio that will allow increasing the number of channels to 8 from 2 in the current system configuration. This could allow using a cuff electrode that has 8 channels to be interfaced with the device for recording the data at 20ksps/channel.

**2. CPLD:** A CPLD could be added as an intermediary between the Intan RHD2216 or RHS2116 and the microcontroller that collects data from the Intan amplifier chip, to avoid any delays in data collection or lost packets due to BLE interruption of the microcontroller.

**3. OAD:** Over the Air Download (OAD) is a feature on the CC2640R2F microcontroller that allows updating the software image wirelessly. This functionality can be added to the existing code to allow a user to update the firmware on the implant module without a physical connection, which will be the case once it is encapsulated. This will allow the system to be more robust and allow improvements to be made even on an implanted device.

# Appendix 1: Device Operation Procedure

This Appendix describes the procedure for using the RHS2116 / RHD2216 implant board and receiver base station for wirelessly recording and stimulating in a nerve. These steps should be followed to ensure proper working of the system.

**Step 1:** Assemble the base station and the implant module system to make it ready for operation. Ensure power is disconnected to both the base station and the implant module.

**Step 2:** Connect the USB cable on the receiver base station to the Host computer and the FPGA board and connect the power cord to the FPGA board.

**Step 3:** Power On the FPGA board.

**Step 4:** Connect the battery to the implant board to power on the implant.

**Step 5:** Bring up the Intan RHD2000 Series modified GUI. Once the GUI opens up, click on the init BLE button in the GUI.

**Step 6:** Observe the Green LED on the Receiver Base Station UWB Module to check if it is blinking and ensure that the Green LED on the CC2640R2-LaunchXL board is turned to green. If not wait until the LED on CC2640R2 turns Red, then click on init BLE again, and check for the Green LED to come up.

**Step 7:** Once the Green LED is lit on the CC2640R2 microcontroller board, wait 15 seconds before clicking on the Run button, to allow proper configuration of the connection

intervals and other parameters like selection of the PHY layer for communication to be setup correctly.

**Step 8:** After 15 seconds click run. Now observe the data coming into the channel 0 and channel 1 of the GUI. If the data is changing, then it is likely that the connection is good. However if there is no data or the data is beyond the normal signal bounds, it is likely that the system did not connect well. In this case, try clicking on Stop and observe the microcontroller board for a red LED to turn off. If the Red LED does not turn off, the connection is not established between the implant and the receiver base station. In which case, power cycle both the implant and the Base station and repeat steps 3 to 8.

**Step 9:** If the data coming on screen looks normal, and control from the base station to the implant module is established, set up the file name in the Intan GUI to which data will be saved. After that click on record.

**Step 10:** Once recording is completed, click on stop, and ensure that the red LED on the CC2640R2-LaunchXL board is turned Off. Now, disconnect the battery on the implant module and disconnect power from the receiver base station.

**Step 11:** Analyze the data.

## Appendix 2: Data rate of Bluetooth Low Energy (BLE)

After performing several tests to find the maximum data rate of Bluetooth Low Energy (BLE) v4.2 and v5.0, several key findings were observed. Below discussion talks about the findings observed from testing a Texas Instruments CC2640R2F BLE v5.0 compatible microcontroller.

1. The maximum allowable data packet size also known as Maximum Transmission Unit (MTU) is 246Bytes.
2. It takes the microcontroller 1.5 ms to send one data packet with 246Bytes across from the transmitter to the receiver.
3. If the MTU is set to the default 23Bytes, data packets can be sent to the receiver every 500us, and that is the lowest achievable transmission time.
4. Running at the maximum capacity, as shown in the BLE v5.0 Throughput code, a maximum data throughput of approx. 1.31Mbps can be achieved (as observed in several tests performed at highest possible throughput rates).

Now looking at these finding, and trying to further understand point 2 from above, if it takes 1.5ms to transmit every data packet, that has a total of 246Bytes of data payload, then

$$8 \times 246 = 1968 \text{ bits}$$

So, 1968 bits are transmitted every 1.5ms, this puts the overall throughput at

$$\frac{1968 \text{ bits}}{1.5 \times 10^{-3} \text{ s}} = 1312 \times 10^3 \text{ bps} = 1.312 \text{ Mbps}$$

That is the same as the maximum data throughput mentioned on the BLE v5.0 protocol.

However, to be able to do that, 246 Bytes of data samples need to be collected and kept ready for transmission. The microcontroller is busy during the 1.5ms as BLE data transmission is occurring, so Intan RHS2116 cannot acquire data samples. So this strategy cannot work for continuous real time data acquisition.

Looking at point 3, sending 23Bytes every 500 $\mu$ s allows some more flexibility, however, it causes the data collection to be interrupted every 500  $\mu$ s. Which means an effective sampling rate of only 2kHz can be achieved for a continuous data sampling system, which is once again too slow for this application.

After extensive tests, it was found that there is no way to send data packets faster than every 500 $\mu$ s, and if more data is acquired and saved for transmitting later, the transmission takes longer which interrupts collection of new data.

This shows that Bluetooth is a good technology to use when discreet data needs to be transferred across devices, like images, or sensor data sets already stored in memory where the sensor acquires data slower than the maximum time it takes to transmit a data packet, but not so much for acquiring and transmitting continuous real-time data.



## Appendix 3: Calculating the Packet Loss Ratio (PLR)

The Packet Loss Ratio (PLR) is calculated by transmitting a predefined data packet that has a packet counter and a series of alternating zeros and ones to the receiver. The packet frame format is shown in Figure 14.

Figure 15 shows the measurement setup environment that is used to perform this test, and Figure 16 shows the actual setup.

Data packets are continuously transmitted from the transmitter and the receiver has an USBee QX logic analyzer connected between the DWM1000 receiver module and the FPGA board. This captures the incoming data packets when they are sent to the FPGA module, and compare it with the data sent from the transmitter. The received packets are analyzed in Microsoft Excel and the results are presented in Table 3.

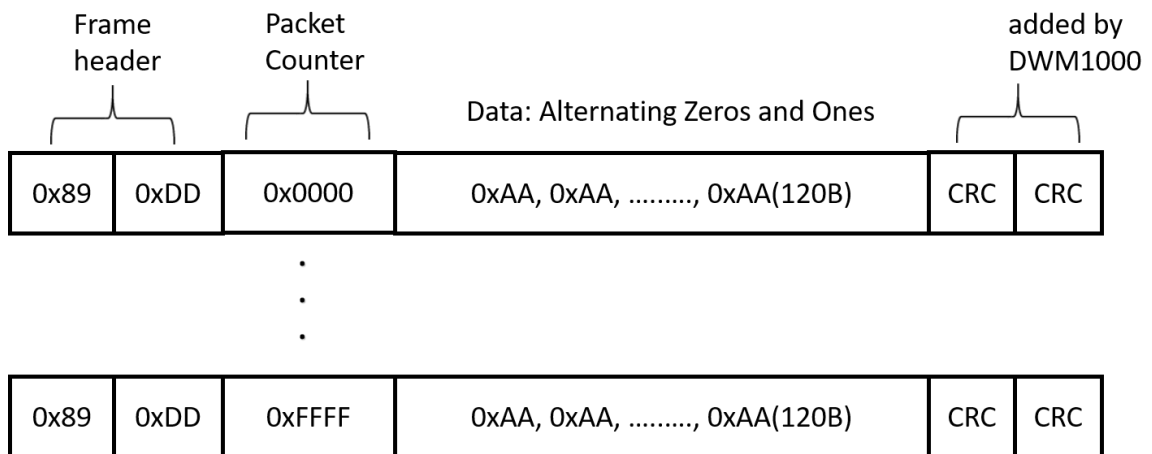


Figure 14 UWB Frame format for Packet Loss Ratio (PLR) calculation

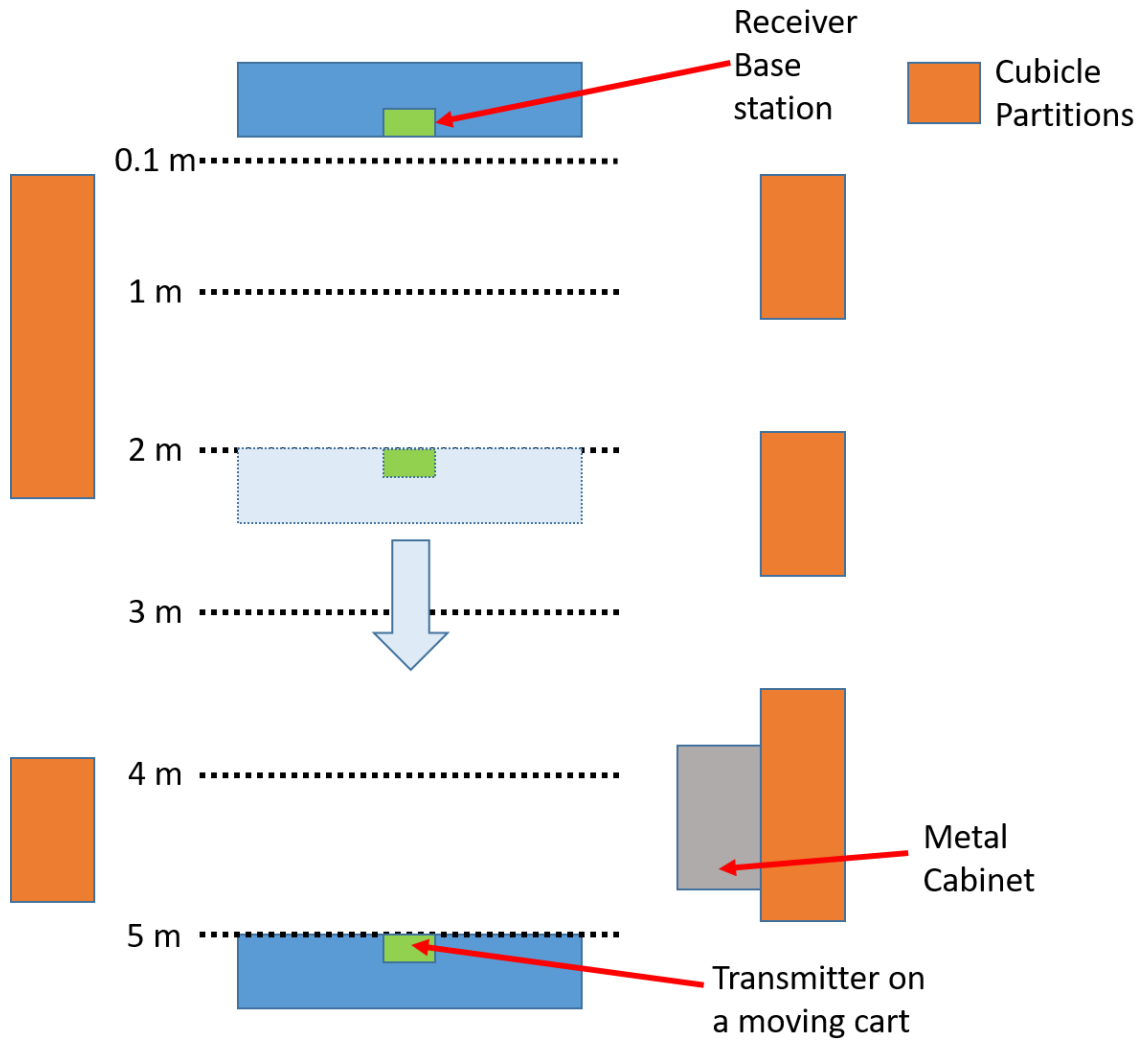
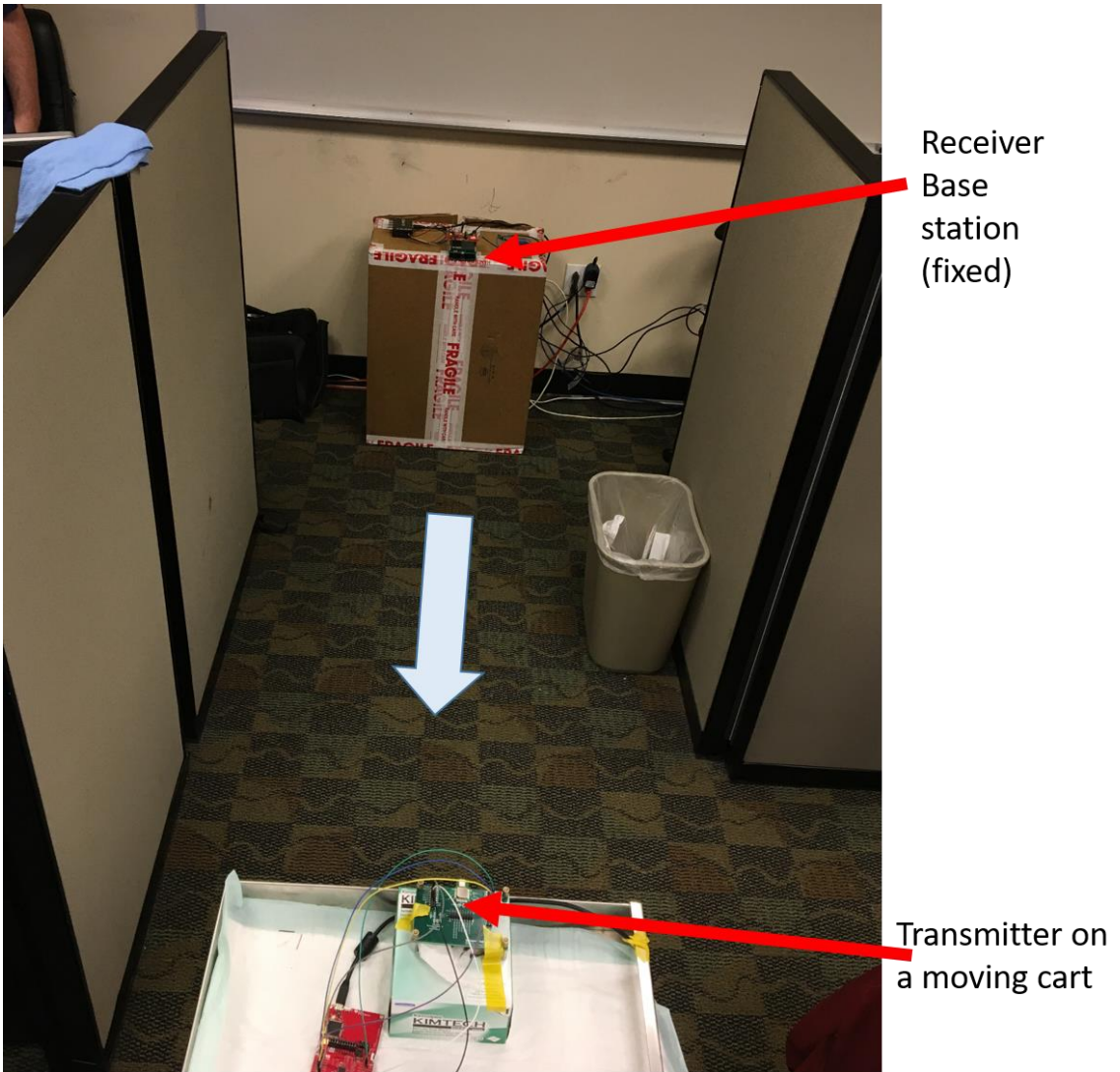


Figure 15 Area layout for the PLR test using a fixed receiver base station and a moving transmitter.



*Figure 16 Actual setup for the Packet Loss ratio (PLR) measurement*

## Appendix 4: Bench Tests on a RHD2216 based transmitter

Before the development of the RHD2216 based recording and stimulating system, bench tests were performed on an earlier prototype for the RHD2216 recording only system. A function generator was used as a signal source for a known fixed amplitude and frequency sine wave signal to validate the programmed filter cut offs, data packet delays and other fine tuning needed before implementing the code on an actual miniature PCB.

Figure 17 shows the test bench layout for performing these tests. The Intan RHD2216 records the data and sends it to the LVDS to CMOS converter, this outputs the signal in CMOS ready to be acquired by the CC2640R2F – LaunchXL board store in the transmit buffer of DWM1000 UWB module which then transmits it to the base station for analysis.

The tests were performed for the below range of Sine Wave Parameters:

**Amplitude range:** 100 $\mu$ V(pp) to 2mV(pp)

**Frequency range:** 100Hz to 5kHz.

Figure 18 (top) shows the observed signals at the base station GUI for an input of 350 $\mu$ V(pp) at 2kHz, and (bottom) shows the signal after passing the input through a bandpass filter between 500Hz to 4kHz.

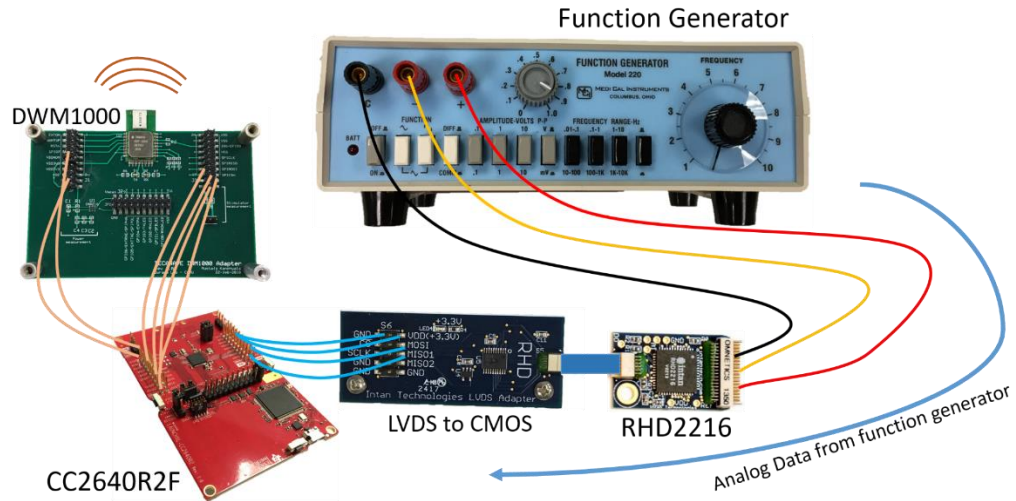


Figure 17: Experimental setup for testing the RHD2216 based recording and transmission system.

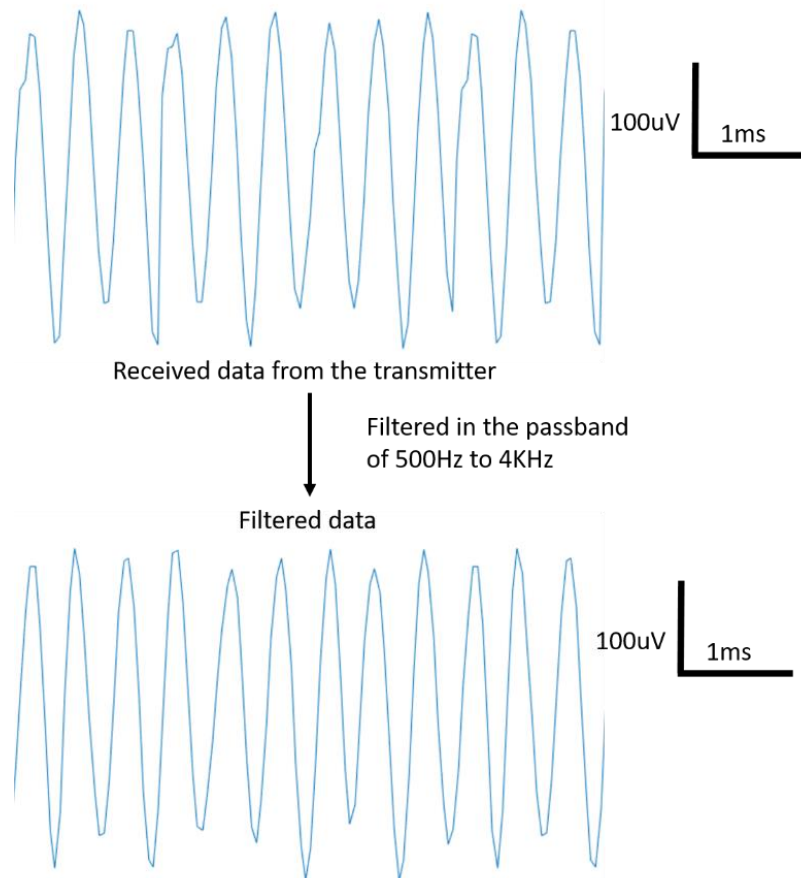


Figure 18: (top) shows the observed signals at the base station GUI for an input of  $350\mu\text{V(pp)}$  at  $2\text{kHz}$ , and (bottom) shows the signal after passing the input through a bandpass filter between  $500\text{Hz}$  to  $4\text{kHz}$ .

## Appendix 5: Bench Tests on RHS2116 for stimulation

To identify the stimulation parameters needed for programming the Intan RHS2116 from the CC2640R2F microcontroller, several tests were performed using the wired Intan RHS2116 system with the Opal Kelly XEM6010 FPGA board, and the Intan Stimulation/Recording Controller v1.04 Software (Intan Technologies LLC). Firstly a custom PCB board for the RHS2116 was built to interface it directly with the FPGA board, to avoid any issues in the Serial Peripheral Interface (SPI) communication (due to CMOS). Then a custom PCB board is built using a TI LP5900 Low Dropout Regulator (LDO) to convert the battery voltage (3.7V) to a regulated 3.3V supply to power the RHS2116 and the TI TPS65133 Dual Output Power Supply to have a  $\pm 5V$  output to provide power to the stimulator on the RHS2116.

A test bench setup as shown in Figure 19 was used, and USBee QX Suite from EE101 was used to store the Serial Peripheral Interface (SPI) data communication between RHS2116 and the Opal Kelly XEM6010 FPGA board. Microsoft Excel was used to analyze the acquired data and processed to identify the configuration parameters. The order in which these commands were sent from the FPGA board were recorded and using that, new configuration parameters were added to program the RHS2116 from the CC2640R2 microcontroller. The results obtained are shown in Figure 20, and a confidence level of about 96% was achieved between the configured parameter and the measured value across a 15 k $\Omega$  resistor that was used to simulate the impedance of a Carbon Nanotube Yarn electrode (CNTY).

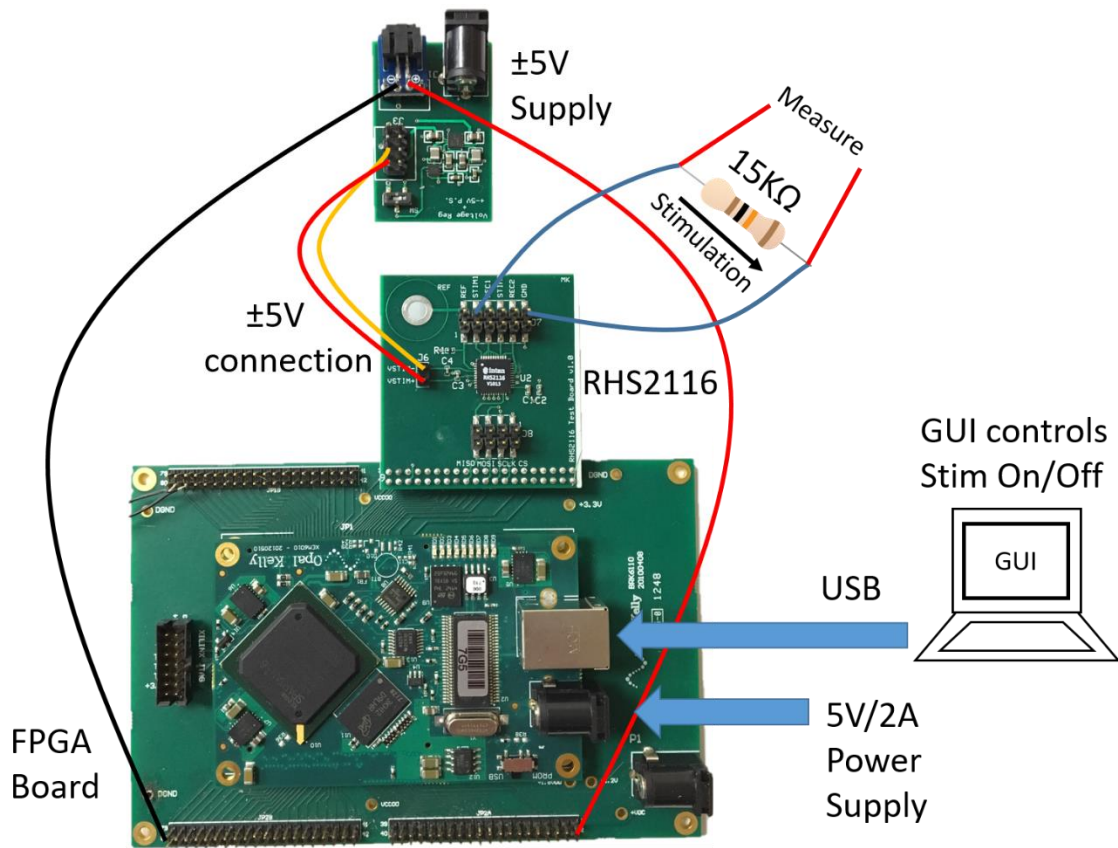


Figure 19 Test bench setup for a wired RHS2116 to identify stimulation parameters needed to stimulate across a 15kΩ resistor to simulate an actual electrode impedance.

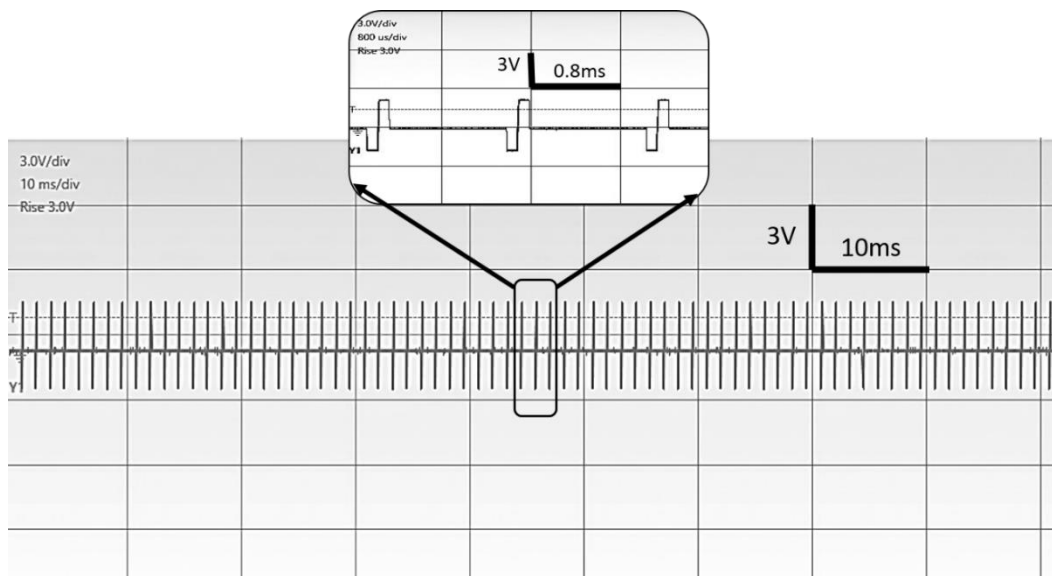


Figure 20 Stimulator output as measured across a 15KΩ resistor to simulate the impedance of a CNTY electrode

## Appendix 6: Circuit Design Layouts

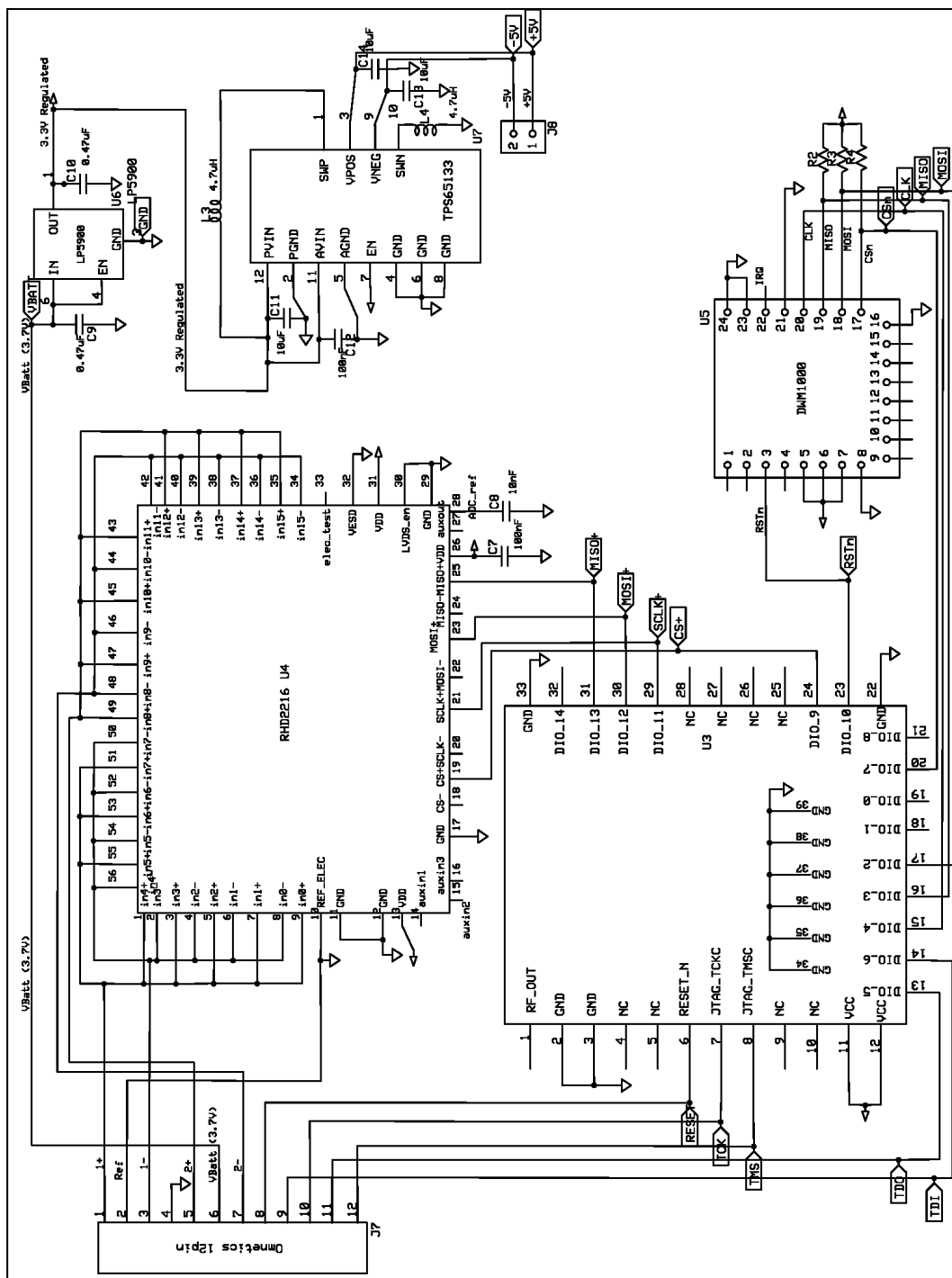


Figure 21: Schematic of the Implant Module for RHD2216



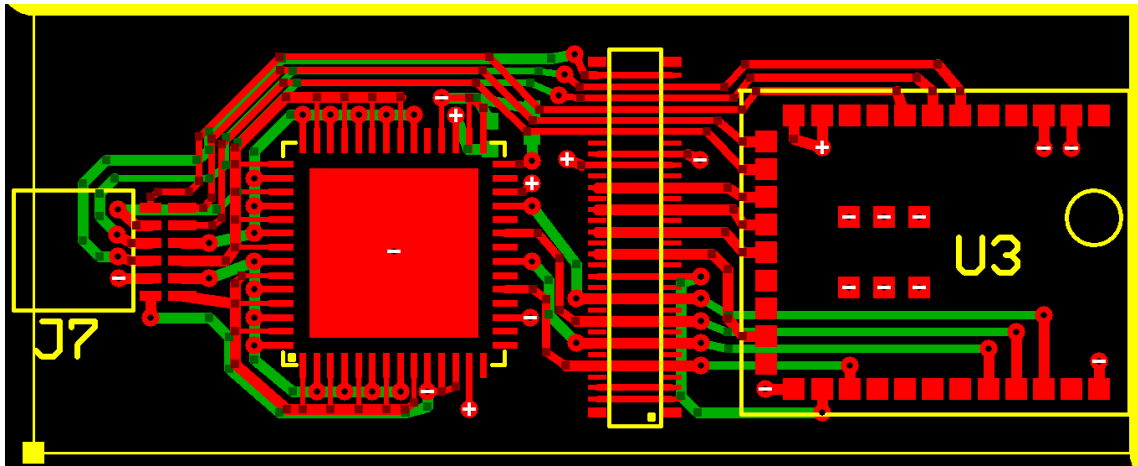


Figure 22: layout of the Bottom PCB layer for the Implant module

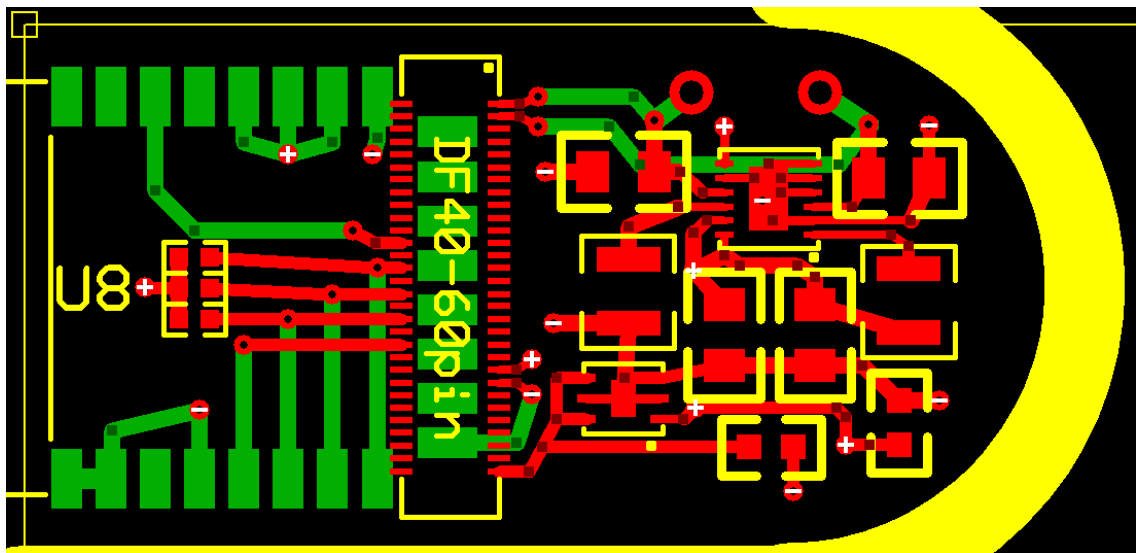
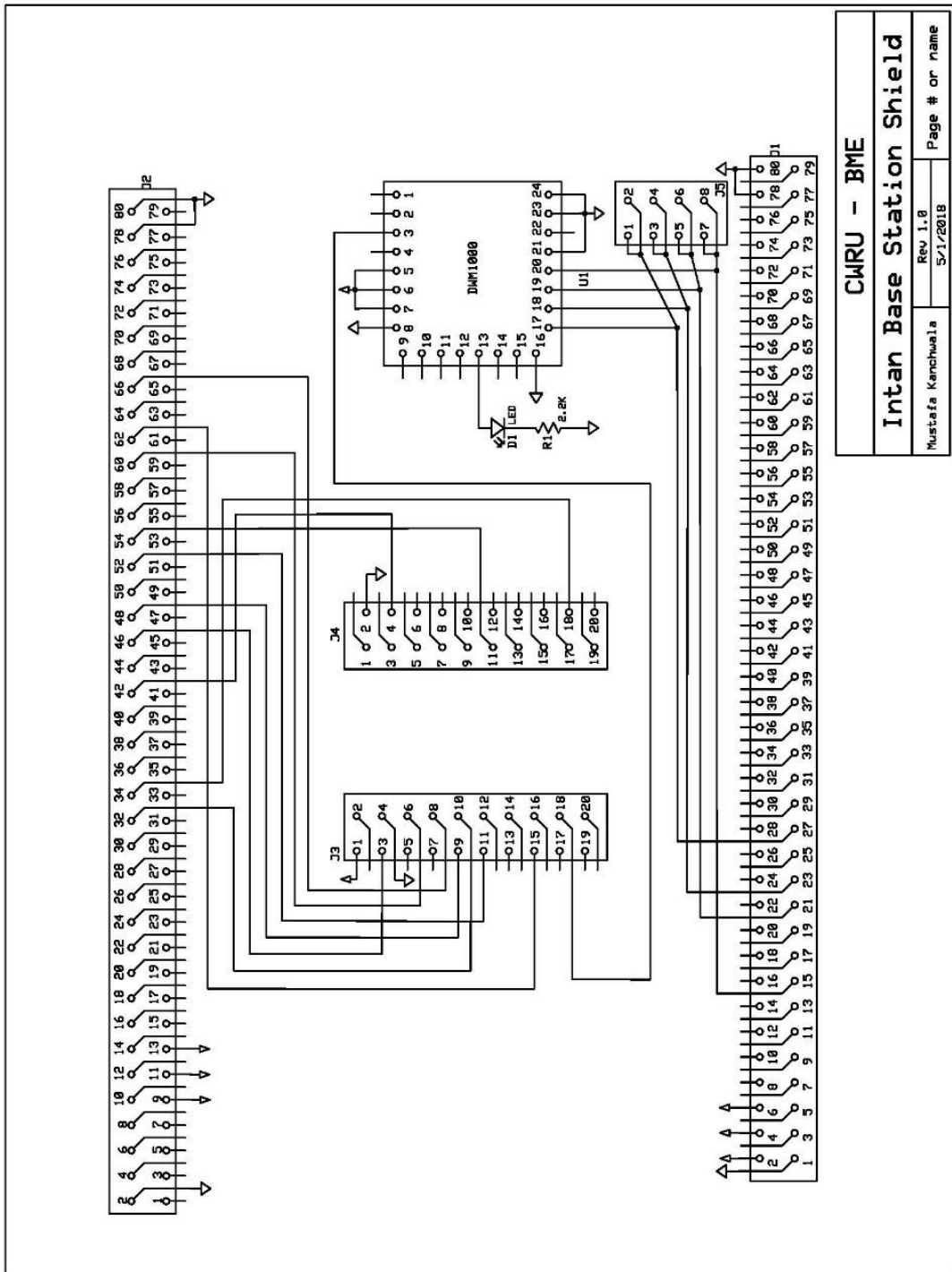


Figure 23: Layout of the Top PCB layer for the Implant Module (\*Top side = Green & Bottom side = Red)



<b>CWRU - BME</b>	
<b>Intan Base Station Shield</b>	
Mustafa Kanchwala	Rev 1.8
S/1/2018	Page # or name

Figure 24: Schematic of the Receiver Base Station Shield Board

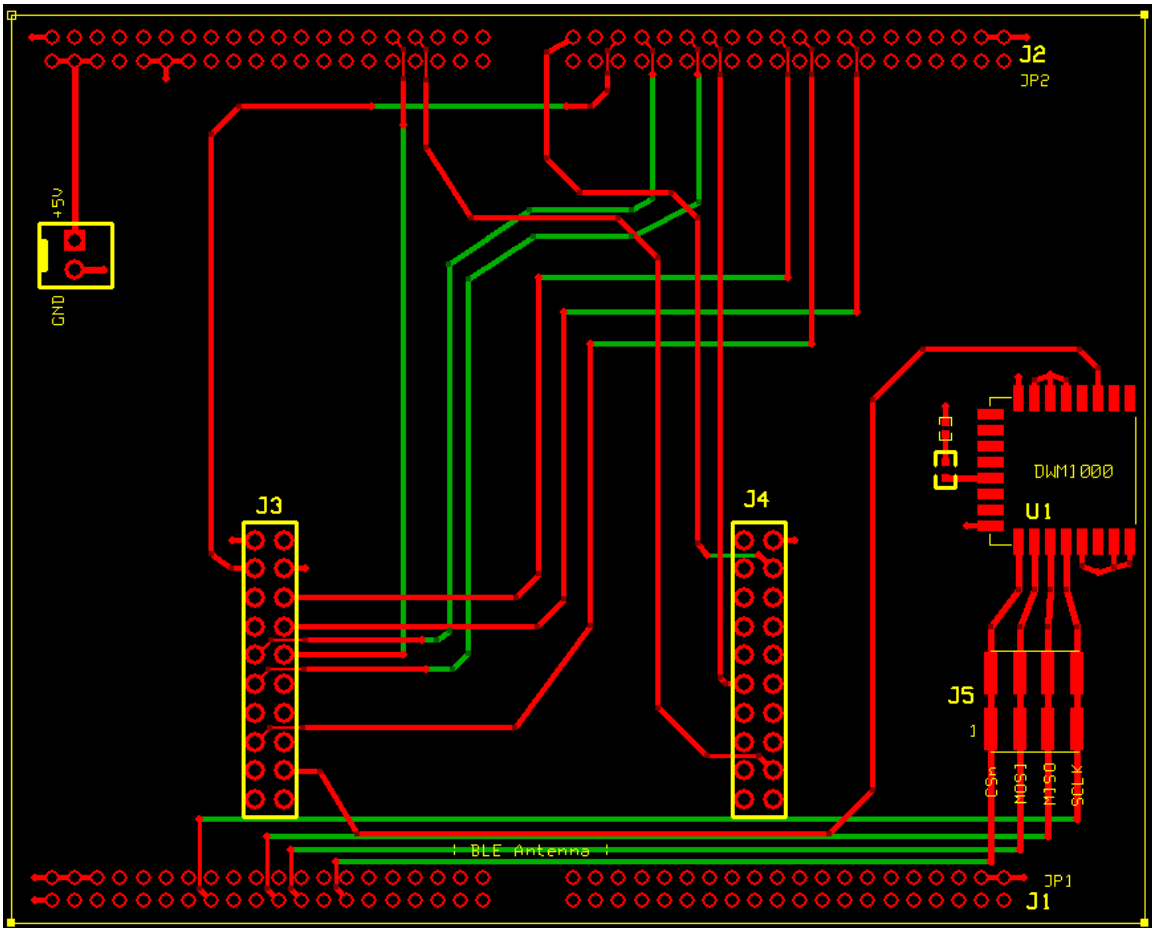


Figure 25: PCB layout of the Base Station Shield Board

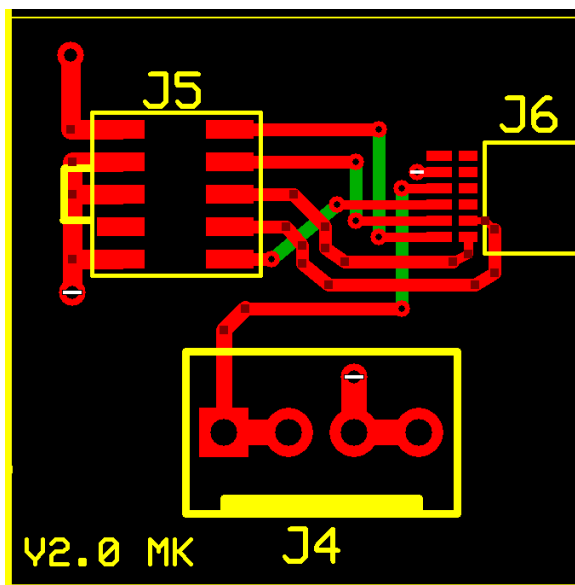


Figure 26: PCB layout of the JTAG to Omnetics Converter Programmer Board

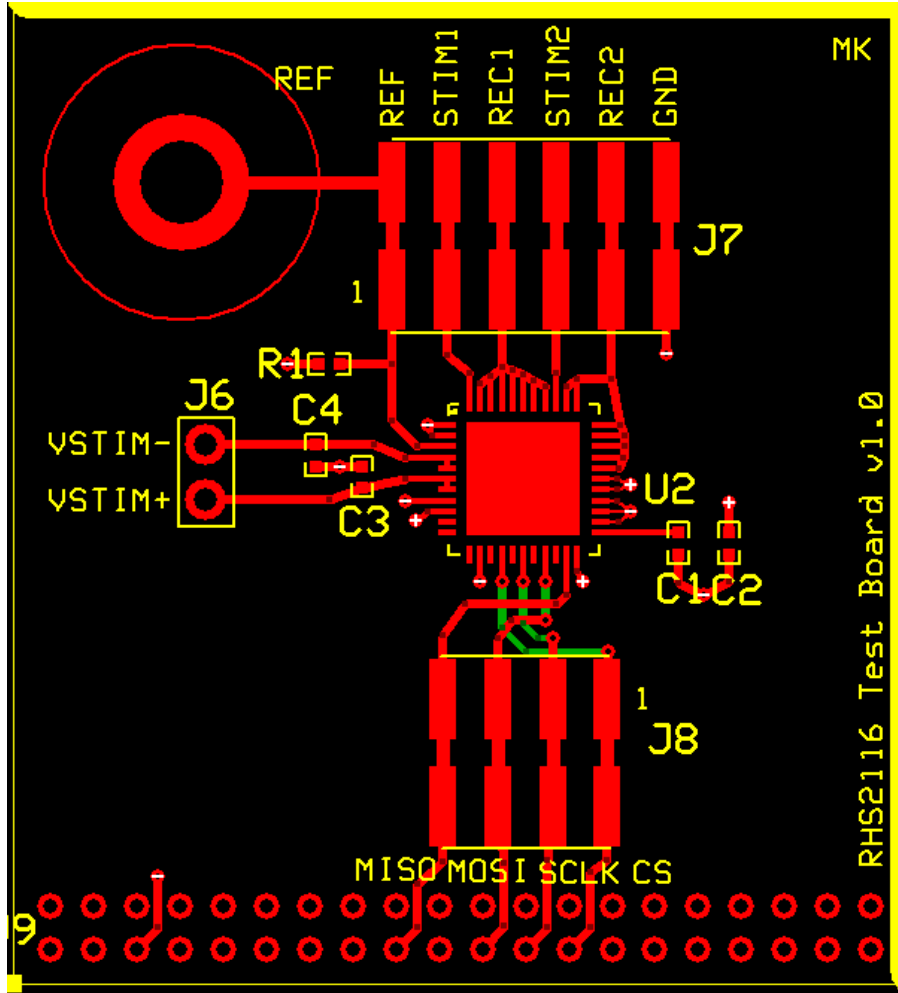


Figure 27: RHS2116 Test Board

## Appendix 7: Source Code and PCB Design Files

The Source code and PCB design files can be found at:

**<https://drive.google.com/open?id=1jljd7ScZIRIC6JM5eke2ucWRJAsStBNN>**

Access to these files can be granted by Dr. Grant McCallum (gam19@case.edu) and Dr. Dominique Durand (dxd6@case.edu) for a reasonable request.

## References

- [1] K. Famm, B. Litt, K. J. Tracey, E. S. Boyden, and M. Slaoui, "Drug discovery: A jump-start for electroceuticals," *Nature*, vol. 496, no. 7444, pp. 159–161, Apr. 2013.
- [2] H. Ekmekçi and H. Kaptan, "Vagal Nerve Stimulation," *Open Access Maced. J. Med. Sci.*, May 2017.
- [3] F. R. Carreno and A. Frazer, "Vagal Nerve Stimulation for Treatment-Resistant Depression," *Neurotherapeutics*, vol. 14, no. 3, pp. 716–727, Jul. 2017.
- [4] S. Gedela, B. Sitwat, W. P. Welch, R. T. Krafty, and Y. Sogawa, "The effect of vagus nerve stimulator in controlling status epilepticus in children," *Seizure*, vol. 55, pp. 66–69, Feb. 2018.
- [5] W. P. Welch, B. Sitwat, and Y. Sogawa, "Use of Vagus Nerve Stimulator on Children With Primary Generalized Epilepsy," *J. Child Neurol.*, vol. 33, no. 7, pp. 449–452, Jun. 2018.
- [6] I. Forde, M. Mansukhani, B. Kolla, and S. Kotagal, "A Potential Novel Mechanism for Vagus Nerve Stimulator-Related Central Sleep Apnea," *Children*, vol. 4, no. 10, p. 86, Sep. 2017.
- [7] Millar, "TR50BB Dual Biopotential Telemeter - Rat | Millar." [Online]. Available: <https://millar.com/products/telemetry/telemeters/TR50BB-dual-biopotential-telemeter>.
- [8] Triangle Biosystems, "W-Series." [Online]. Available: <https://www.trianglebiosystems.com/w-series-systems.html>.
- [9] G. Charvet *et al.*, "WIMAGINE®: 64-channel ECoG recording implant for human applications," *Proc. Annu. Int. Conf. IEEE Eng. Med. Biol. Soc. EMBS*, pp. 2756–2759, 2013.
- [10] C. S. Mestais, G. Charvet, F. Sauter-Starace, M. Foerster, D. Ratel, and A. L. Benabid, "WIMAGINE: Wireless 64-Channel ECoG Recording Implant for Long Term Clinical Applications," *IEEE Trans. Neural Syst. Rehabil. Eng.*, vol. 23, no. 1, pp. 10–21, Jan. 2015.
- [11] R. E. Hampson, V. Collins, and S. A. Deadwyler, "Transmit Neural Activity in Freely Moving Animals," *J. Neurosci.*, vol. 182, no. 2, pp. 195–204, 2010.
- [12] M. HIRATA *et al.*, "A Fully-Implantable Wireless System for Human Brain-Machine Interfaces Using Brain Surface Electrodes: W-HERBS," *IEICE Trans. Commun.*, vol. E94–B, no. 9, pp. 2448–2453, 2011.
- [13] R. E. Hampson, V. Collins, and S. A. Deadwyler, "A wireless recording system that

utilizes Bluetooth technology to transmit neural activity in freely moving animals,” *J. Neurosci. Methods*, vol. 182, no. 2, pp. 195–204, Sep. 2009.

- [14] “Bluetooth 5 - Go Faster. Go Further. | Bluetooth Technology Website.” [Online]. Available: <https://www.bluetooth.com/bluetooth-technology/bluetooth5/bluetooth5-paper>.
- [15] H. Ando, K. Takizawa, T. Yoshida, K. Matsushita, M. Hirata, and T. Suzuki, “Wireless Multichannel Neural Recording with a 128-Mbps UWB Transmitter for an Implantable Brain-Machine Interfaces,” *IEEE Trans. Biomed. Circuits Syst.*, vol. 10, no. 6, pp. 1068–1078, Dec. 2016.
- [16] M. S. Chae, Z. Yang, M. R. Yuce, L. Hoang, and W. Liu, “A 128-channel 6 mW wireless neural recording IC with spike feature extraction and UWB transmitter,” *IEEE Trans. Neural Syst. Rehabil. Eng.*, vol. 17, no. 4, pp. 312–321, 2009.
- [17] E. Greenwald, M. Mollazadeh, C. Hu, W. Tang, E. Culurciello, and N. Thakor, “A VLSI neural monitoring system with ultra-wideband telemetry for awake behaving subjects,” *IEEE Trans. Biomed. Circuits Syst.*, vol. 5, no. 2, pp. 112–119, 2011.
- [18] A. Demosthenous, “Advances in Microelectronics for Implantable Medical Devices,” *Adv. Electron.*, vol. 2014, pp. 1–21, 2014.
- [19] Intan Technologies, “RHS2116 Digital Electrophysiology Stimulator/Amplifier Chip,” 2016. [Online]. Available: [http://intantech.com/files/Intan\\_RHS2116\\_datasheet.pdf](http://intantech.com/files/Intan_RHS2116_datasheet.pdf).
- [20] G. A. McCallum *et al.*, “Chronic interfacing with the autonomic nervous system using carbon nanotube (CNT) yarn electrodes,” *Sci. Rep.*, vol. 7, no. 1, pp. 1–14, 2017.
- [21] Texas Instruments, “CC2640R2F CC2640R2F SimpleLink™ Bluetooth® low energy Wireless MCU 1 Device Overview.” [Online]. Available: <http://www.ti.com/lit/ds/symlink/cc2640r2f.pdf>.
- [22] Y. M. Dweiri, T. Eggers, G. McCallum, and D. M. Durand, “Ultra-low noise miniaturized neural amplifier with hardware averaging,” *J. Neural Eng.*, vol. 12, no. 4, 2015.
- [23] DecaWave, “Product Overview DWM1000.” [Online]. Available: <https://decawave.com/sites/default/files/dwm1000-datasheet-v1.6.pdf>. [Accessed: 13-Jun-2018].
- [24] Opal Kelly, “XEM6010 - Opal Kelly.” [Online]. Available: <https://www.opalkelly.com/products/xem6010/>.
- [25] Laird Technologies, “SaBLE-x Bluetooth Low Energy (BLE) Module.” [Online]. Available: <https://www.lsr.com/embedded-wireless-modules/bluetooth-module/sable-x-ble-module>.

- [26] IEEE, "IEEE 802.15.4-2011 - IEEE Standard for Local and metropolitan area networks--Part 15.4: Low-Rate Wireless Personal Area Networks (LR-WPANs)." [Online]. Available: <https://standards.ieee.org/findstds/standard/802.15.4-2011.html>.
- [27] Texas Instruments, "LP5900 LP5900 150-mA Ultra-Low-Noise LDO for RF and Analog Circuits - Requires No Bypass Capacitor," 2005. [Online]. Available: <http://www.ti.com/lit/ds/symlink/lp5900.pdf>.
- [28] Texas Instruments, "TPS65133 Split-Rail Converter,  $\pm 5V$ , 250mA Dual Output Power Supply | TI.com." [Online]. Available: <http://www.ti.com/product/TPS65133>.
- [29] Texas Instruments, "INA216 5V, Low-Power, High-side, Zero-Drift, Voltage Output Current Sense Amp in WCSP package | TI.com." [Online]. Available: <http://www.ti.com/product/INA216>.
- [30] Texas Instruments, "BLE-Stack APIs: Codec1.h File Reference." [Online]. Available: [http://dev.ti.com/tirex/content/simplelink\\_cc2640r2\\_sdk\\_1\\_30\\_00\\_25/docs/blestack/ble\\_sw\\_dev\\_guide/doxygen/\\_codec1\\_8h.html](http://dev.ti.com/tirex/content/simplelink_cc2640r2_sdk_1_30_00_25/docs/blestack/ble_sw_dev_guide/doxygen/_codec1_8h.html).
- [31] Texas Instruments, "Creating a Voice Enabled Application — Bluetooth Low Energy Software Developer's Guide 3.00.01 documentation." [Online]. Available: [http://dev.ti.com/tirex/content/simplelink\\_cc2640r2\\_sdk\\_1\\_35\\_00\\_33/docs/blestack/ble\\_sw\\_dev\\_guide/html/voice/voice.html](http://dev.ti.com/tirex/content/simplelink_cc2640r2_sdk_1_35_00_33/docs/blestack/ble_sw_dev_guide/html/voice/voice.html).